

INFLAMMATORY BOWEL DISEASE

Heterogeneity and clonal relationships of adaptive immune cells in ulcerative colitis revealed by single-cell analyses

Brigid S. Boland^{1*}, Zhaoren He^{2,3*}, Matthew S. Tsai^{1*}, Jocelyn G. Olvera¹, Kyla D. Omilusik³, Han G. Duong¹, Eleanor S. Kim¹, Abigail E. Limary¹, Wenhao Jin², J. Justin Milner³, Bingfei Yu³, Shefali A. Patel¹, Tiani L. Louis¹, Tiffani Tysl¹, Nadia S. Kurd^{1†}, Alexandra Bortnick³, Lauren K. Quezada¹, Jad N. Kanbar¹, Ara Miralles¹, Danny Huylebroeck^{4,5}, Mark A. Valasek⁶, Parambir S. Dulai¹, Siddharth Singh¹, Li-Fan Lu³, Jack D. Bui⁶, Cornelis Murre³, William J. Sandborn¹, Ananda W. Goldrath³, Gene W. Yeo^{2,7‡}, John T. Chang^{1,8‡}

Copyright © 2020
The Authors, some
rights reserved;
exclusive licensee
American Association
for the Advancement
of Science. No claim
to original U.S.
Government Works

Inflammatory bowel disease (IBD) encompasses a spectrum of gastrointestinal disorders driven by dysregulated immune responses against gut microbiota. We integrated single-cell RNA and antigen receptor sequencing to elucidate key components, cellular states, and clonal relationships of the peripheral and gastrointestinal mucosal immune systems in health and ulcerative colitis (UC). UC was associated with an increase in IgG1⁺ plasma cells in colonic tissue, increased colonic regulatory T cells characterized by elevated expression of the transcription factor ZEB2, and an enrichment of a $\gamma\delta$ T cell subset in the peripheral blood. Moreover, we observed heterogeneity in CD8⁺ tissue-resident memory T (T_{RM}) cells in colonic tissue, with four transcriptionally distinct states of differentiation observed across health and disease. In the setting of UC, there was a marked shift of clonally related CD8⁺ T_{RM} cells toward an inflammatory state, mediated, in part, by increased expression of the T-box transcription factor Eomesodermin. Together, these results provide a detailed atlas of transcriptional changes occurring in adaptive immune cells in the context of UC and suggest a role for CD8⁺ T_{RM} cells in IBD.

INTRODUCTION

Inflammatory bowel disease (IBD) encompasses a spectrum of complex intestinal disorders characterized by dysregulated innate and adaptive immune responses to gut microbiota in genetically susceptible hosts (1). IBD is typically categorized as Crohn's disease or ulcerative colitis (UC) on the basis of anatomic, clinical, and histopathologic criteria (2). A number of studies aimed at uncovering the cellular and molecular basis of IBD have been undertaken, thereby implicating a number of diverse immune cell types in its pathogenesis, such as macrophages (3, 4), innate lymphoid cells (5–7), and subsets of CD4⁺ T cells (8–10). The vast majority of gene expression analyses in IBD have used whole intestinal tissue or bulk populations of cells fluorescence-activated cell sorting (FACS)-purified from peripheral blood or intestinal tissue on the basis of phenotypic cell surface markers. However, intestinal tissue is heterogeneous, composed of diverse epithelial, stromal, and immune cells, and it has been increasingly appreciated that substantial heterogeneity can exist even within the same immune cell type (11, 12). Thus, gene expression measurements of whole-tissue samples likely detect the most highly

expressed mRNA transcripts in the most abundant cells, thereby masking many potentially important cell type-specific transcriptional signatures.

Emerging data from a number of laboratories across many fields have demonstrated the necessity and power of an unbiased, marker-agnostic approach in investigating known cell types and discovering previously unidentified cell subsets and states (11–16). In particular, single-cell RNA sequencing (scRNA-seq) has been used to investigate the heterogeneity of intestinal cells in the context of IBD (17–20). In addition to transcriptomic analyses, the ability to delineate T cell (scTCR-seq) and B cell (scBCR-seq) receptor sequences at the single-cell level has enabled characterization of TCR and BCR repertoire diversity and identification of clonal relationships (21, 22). Together, these studies have generated exciting insights that could only have been revealed by analyses performed at the single-cell level.

Here, we integrated scRNA-seq, scTCR-seq, and scBCR-seq approaches to elucidate key components, cellular states, and clonal relationships of the gastrointestinal mucosal and peripheral immune systems in health and UC. Substantial heterogeneity among T and B cell subsets was observed, including within plasma B cells, gamma delta ($\gamma\delta$) T cells, regulatory T (T_{reg}) cells, and CD8⁺ tissue-resident memory T (T_{RM}) cells. It is well established that T_{RM} cells mediate protective responses to microbial infection (23), but a potentially pathogenic role for these cells in autoimmune and inflammatory diseases has been increasingly appreciated (24, 25). We observed clonally related CD8⁺ T_{RM} cells in four putative differentiation states across health and disease. In UC, CD8⁺ T_{RM} cells exhibited a marked shift toward an inflammatory differentiation state associated with increased expression of the T-box transcription factor Eomesodermin (Eomes). By virtue of binding to gene targets encoding molecules with inflammatory and effector properties, such as cytokines, cytolytic granules, and

¹Department of Medicine, University of California, San Diego, La Jolla, CA, USA.

²Department of Cellular and Molecular Medicine, University of California, San Diego, La Jolla, CA, USA.

³Division of Biologic Sciences, University of California, San Diego, La Jolla, CA, USA.

⁴Department of Development and Regeneration, University of Leuven, Leuven, Belgium.

⁵Department of Cell Biology, Erasmus University Medical Center Rotterdam, 3015 CN Rotterdam, Netherlands.

⁶Department of Pathology, University of California, San Diego, La Jolla, CA, USA.

⁷Institute for Genomic Medicine, University of California, San Diego, La Jolla, CA, USA.

⁸Division of Gastroenterology, VA San Diego Healthcare System, San Diego, CA, USA.

*These authors contributed equally to this work.

†Present address: Cancer Immunology Discovery, Pfizer Oncology Research and Development, La Jolla, CA 92121, USA.

‡Corresponding author. Email: changj@ucsd.edu (J.T.C.); geneyeo@ucsd.edu (G.W.Y.).

killer cell lectin receptors, Eomes may be a critical molecular regulator of a pathogenic CD8⁺ T_{RM} cell differentiation state in UC.

RESULTS

Single-cell profiling of human immune cells from peripheral blood and colon

UC affects the rectum in the vast majority of cases, and inflammation extends proximally in a contiguous manner. This uniformity enabled us to sample this same region in every participant and minimize potential nonbiologic sources of variability, such as regional differences along the gastrointestinal tract and variable exposures to luminal contents. To probe for transcriptional signatures that might be specific to health or disease, we obtained rectal mucosal biopsy and peripheral blood samples from nine healthy individuals and seven patients with active UC (Fig. 1A and table S2). Cells from mucosal biopsies and peripheral blood were processed into single-cell suspensions, FACS-purified on the basis of CD45, a pan-immune cell marker (fig. S1A), and subjected to scRNA-seq, scTCR-seq, and scBCR-seq using the 10x Genomics Chromium platform.

Two thousand, one hundred sixteen genes with a mean expression of at least 1 UPM (unique molecular identifier per million reads) were detected, with a total of 10,160 genes detected across the dataset (fig. S1, B and C, and table S3). Data from all participants across both anatomic sites were merged, and unsupervised *t*-distributed stochastic neighborhood embedding (*t*-SNE) analysis was performed to visualize the clustering of single cells from all participants (Fig. 1B). We used expression of canonical genes (see Materials and Methods) to annotate the clusters into four broad groups of immune cell types: T lymphocytes, B lymphocytes, natural killer (NK) cells, and myeloid cells. No substantial differences in the proportions of each major immune cell group were observed between healthy individuals and patients with UC (Fig. 1C), nor was the level of overall BCR or TCR repertoire diversity notably different between healthy individuals and patients with UC (fig. S1, D and E).

Transcriptionally distinct immunoglobulin G1-positive plasma cell cluster enriched in UC

Additional *t*-SNE and uniform manifold approximation and projection (UMAP)

clustering analyses were performed on B lymphocytes, yielding 17 subclusters, all of which included cells from at least two participants (Fig. 2, A and B; fig. S2, A to E; and table S3). B cell clusters were broadly categorized into naïve, memory, or plasma cell clusters on the basis of differential expression of canonical genes. For example, naïve and memory cells expressed high levels of genes such as *CD19* and could be further annotated as naïve (clusters B3, B8, and B9) or memory (clusters B2, B4, and B5) on the basis of high or low expression

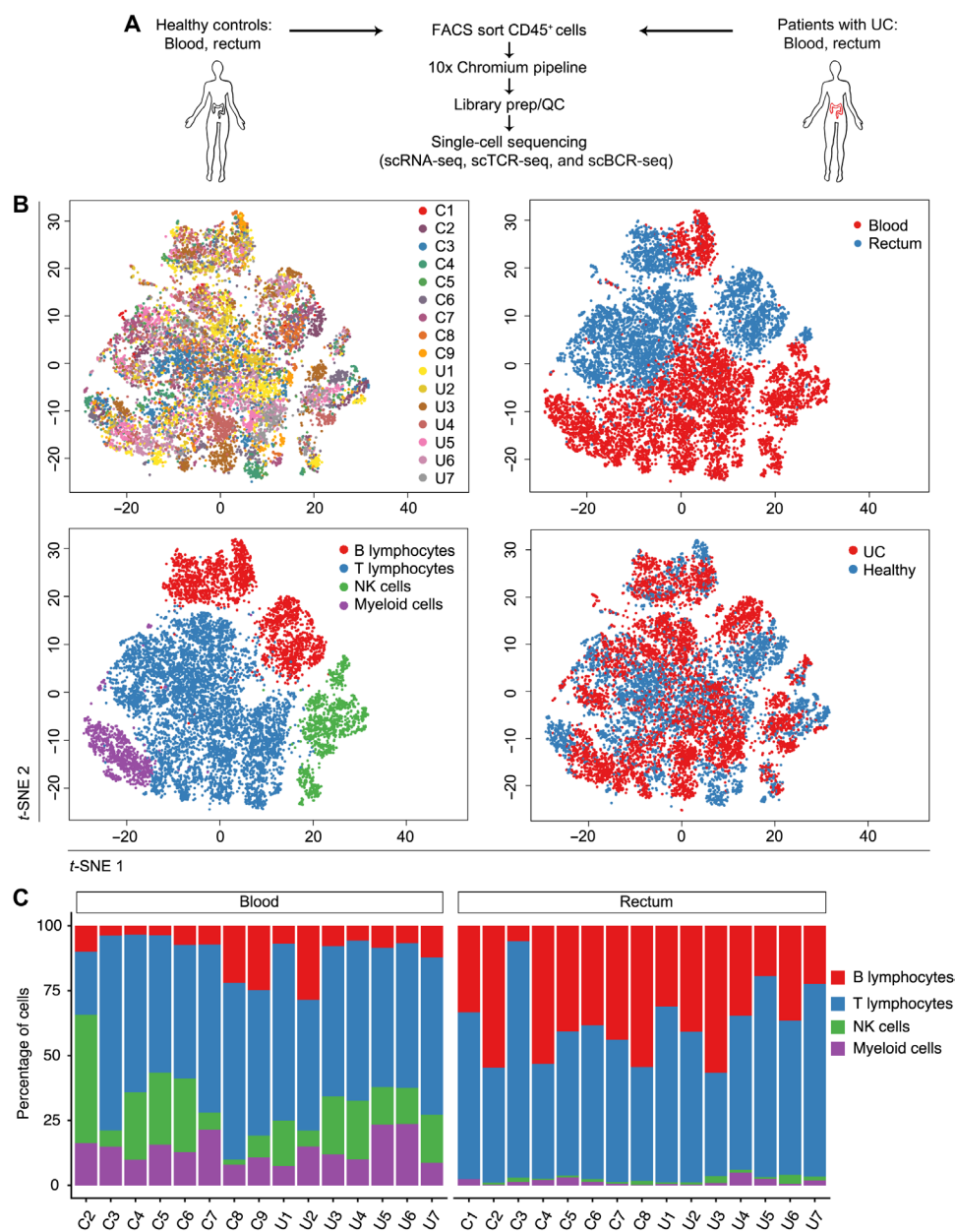


Fig. 1. Single-cell analyses reveal cellular composition of the human immune system in health and UC. (A) Overview of the experimental design and analysis. QC, quality control. (B) *t*-SNE plots of cells from all participants across all anatomic sites (upper left; “C” labels indicate healthy controls and “U” labels indicate patients with UC), colored by anatomic location from which cells were derived (upper right) and major immune cell groups (lower left) or by health status (lower right; patients with UC versus healthy individuals). (C) Proportion of each major immune cell group in healthy individuals and patients with UC, across both anatomic sites for each participant, as a percentage of all cells.

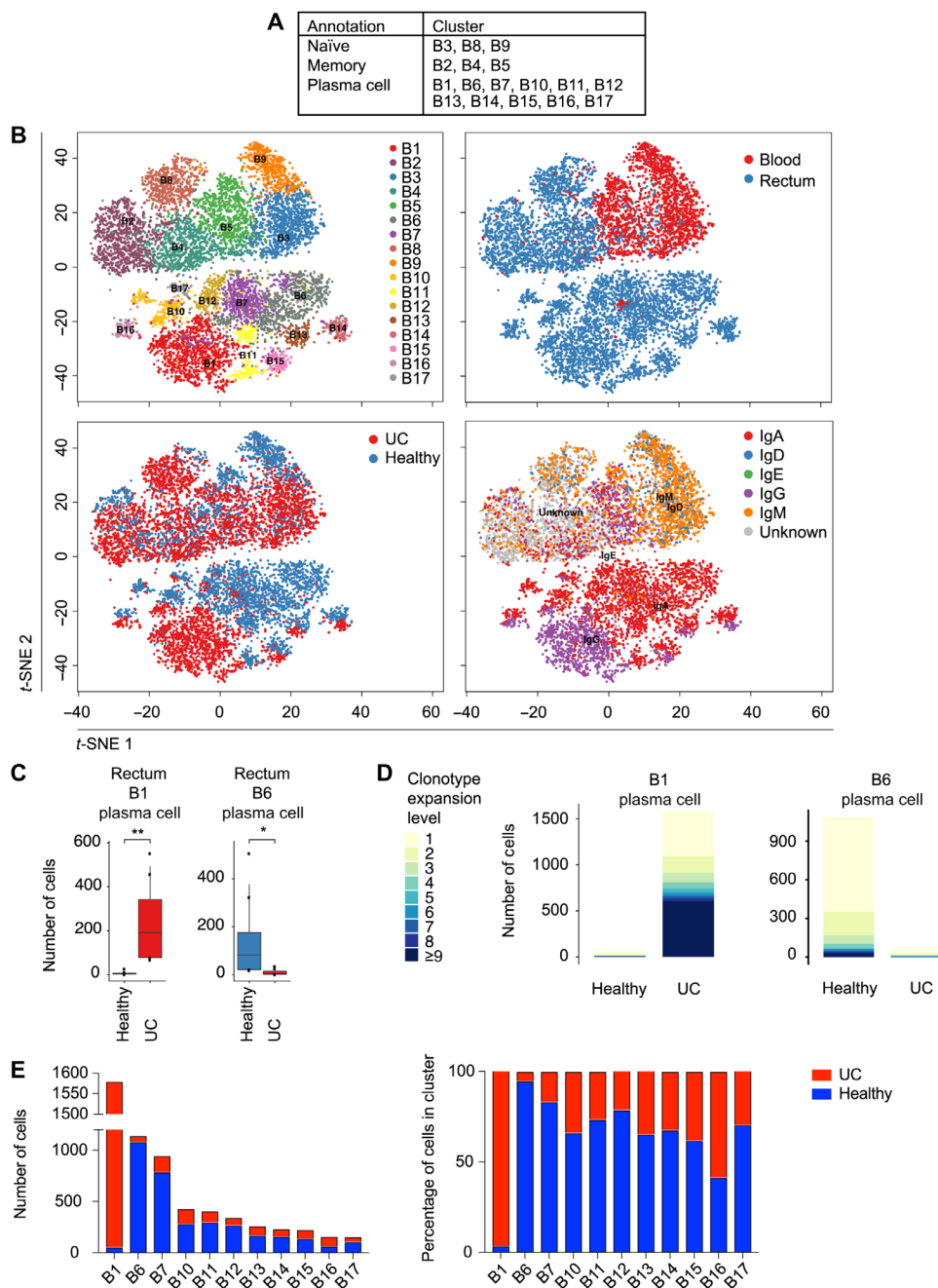


Fig. 2. Enrichment and clonal expansion of an intestinal plasma B cell cluster in UC. (A) Phenotypic annotations of B lymphocyte clusters. (B) t-SNE plots of B lymphocyte clusters, colored by cluster identity (upper left), anatomic location from which cells were derived (upper right), health status (lower left), and immunoglobulin heavy chain expression, determined using scBCR-seq data (lower right). (C) Quantitation of selected B lymphocyte clusters enriched or depleted in health versus disease, expressed as absolute numbers. (D) Comparison of clonotypic expansion exhibited by cells from indicated plasma cell clusters, quantitated separately in healthy individuals versus patients with UC. (E) Absolute number (left) and percentage of cells (right) from each cluster derived from healthy individuals (blue) or patients with UC (red). Two-sided Wilcoxon rank sum test (C). * $P < 0.05$ and ** $P < 0.01$.

of *IGHD*, respectively. Eleven plasma cell clusters were identified on the basis of high expression of *PRDM1* and *XBP1*. Many clusters exhibited strong anatomic associations; only three clusters, the B3 and B9 naïve clusters and the B5 memory cluster, were found

predominantly in the peripheral blood, whereas the rest of the B cell clusters were found preferentially in the intestinal tissue (Fig. 2B and fig. S2, F and G). We next compared the absolute and relative numbers of each cluster in the healthy and disease states. The B1 plasma cell cluster was almost exclusively derived from patients with UC, and cells from this cluster were observed to have undergone increased clonal expansion in patients with UC, whereas the B6 plasma cell cluster was highly enriched in healthy individuals, and cells from this cluster were observed to have undergone clonal expansion preferentially in healthy individuals (Fig. 2, C to E, and fig. S2G).

To begin to explore the molecular basis of the heterogeneity among the plasma cell clusters, we performed differential expression analyses among the 11 plasma cell clusters. The UC-enriched B1 cluster exhibited 165 differentially expressed genes compared with all other plasma cell clusters (table S4). Moreover, we observed that cells from the UC-enriched B1 cluster were predominantly immunoglobulin G1 positive (IgG1^+) (Fig. 3A); additional analyses indicated that the number and proportion of IgG1^+ plasma cells were markedly increased in patients with UC, whereas the number and proportion of IgA2^+ plasma cells were increased in healthy individuals (Fig. 3B). Last, we looked for evidence of BCR clonotypes shared among the B cell clusters that we annotated. In the healthy setting, clonotypes were shared across multiple plasma cell clusters, but not the B1 plasma cell cluster (Fig. 3C, left, and fig. S3A). By contrast, in the setting of UC, clonotypes were shared between cells from the B1 plasma cell cluster and most other plasma cell clusters. Together, these results suggest the possibility that plasma cells transit between distinct states, the relative proportions of which differ in the setting of health versus disease.

Transcriptionally distinct T_{reg} cells in health versus UC

Analogous to our B lymphocyte analyses, additional t-SNE and UMAP analyses were performed on T lymphocytes, yielding 17 subclusters, all of which included cells from at least two participants (Fig. 4, A and B; fig. S4, A to F; and table S3). These T cell clusters were annotated into subsets on the basis of differential expression of canonical genes.

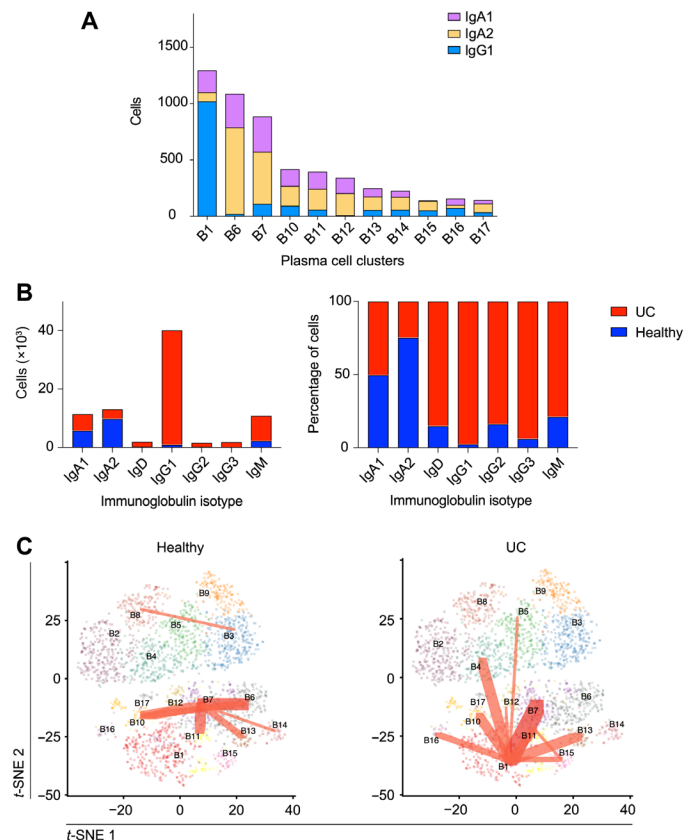


Fig. 3. Clonal relationships of intestinal plasma B cell clusters in health and UC. (A) Quantitation of IgA1⁺, IgA2⁺, and IgG1⁺ cells within each plasma cell cluster, determined using scBCR-seq data. (B) Absolute number and percentage of cells from patients with UC or healthy individuals are shown for each immunoglobulin isotype (IgA1⁺, IgA2⁺, IgD⁺, IgG1⁺, IgG2⁺, and IgM⁺ only; very few IgG3⁺, IgG4⁺, or IgE⁺ cells were detected). (C) t-SNE plots of plasma cell clusters, colored by cluster identity, with red lines indicating BCR clonotypes shared among clusters and line weight representing number of shared clonotypes, for healthy individuals (left) versus patients with UC (right).

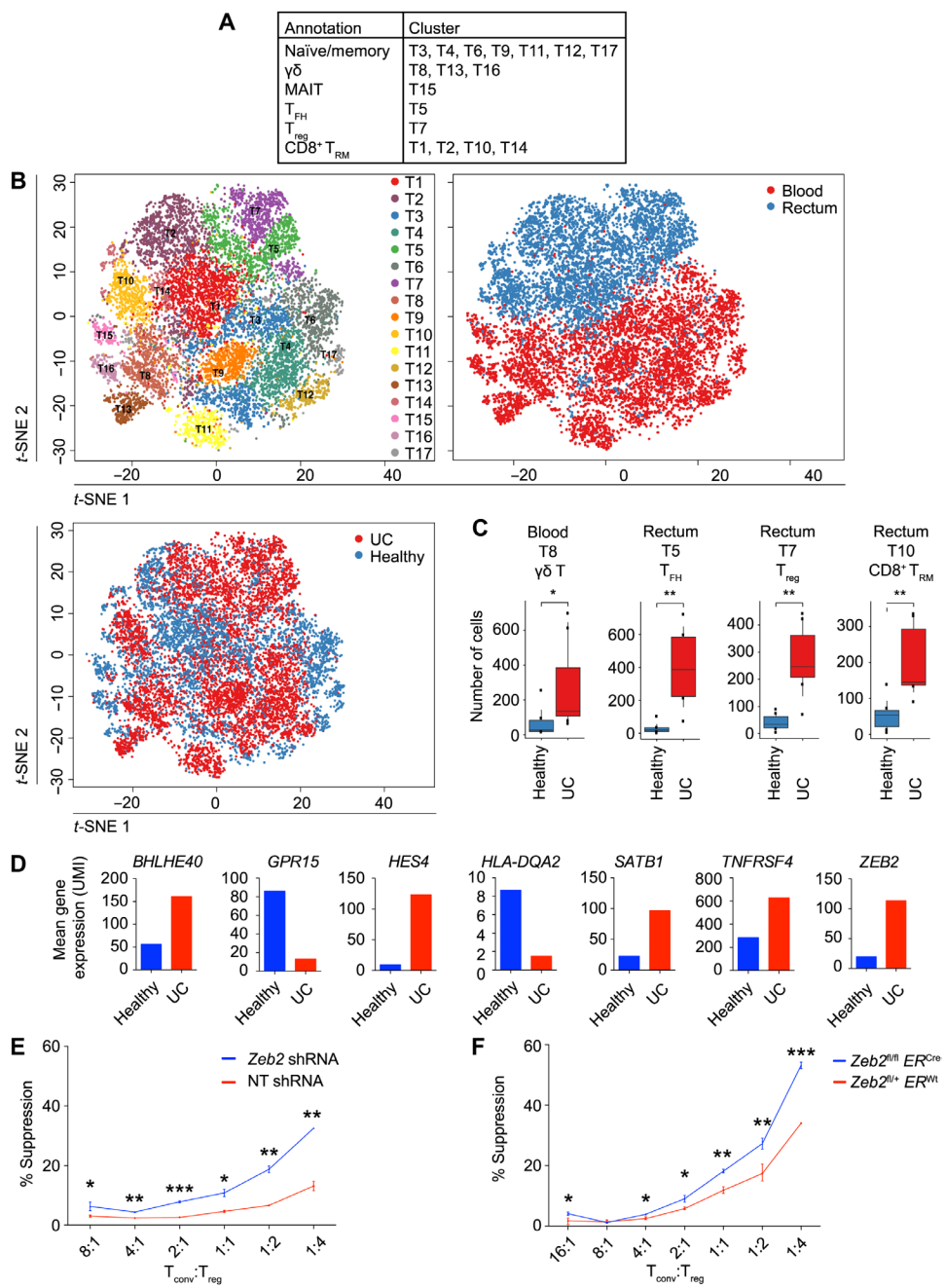
Cells from three clusters (T8, T13, and T16) exhibited high expression of genes encoding components of the $\gamma\delta$ TCR, although it should be noted that the T8 cluster also contained TCR alpha beta ($\alpha\beta$) T cells. Seven clusters (T3, T4, T6, T9, T11, T12, and T17) with high expression of *SELL* (CD62L), *CCR7*, *LEF1*, and *TCF7* were annotated as naïve/memory. Four CD8⁺ T cell clusters (T1, T2, T10, and T14) expressed transcripts suggestive of a T_{RM} cell phenotype (23), with high expression of *CD69*, *ITGAE* (CD103), *CD101*, *CCR6*, and *ITGA1* (CD49a) along with low expression of *KLF2* and *SIPRI1*. Cells from the T7 cluster expressed transcripts indicative of T_{reg} cells (26), including high *FOXP3* and *IL2RA* (CD25) expression along with low *IL7R* expression. Cells from the T5 cluster expressed transcripts suggestive of T follicular helper (T_{FH}) cells (27), including high *CXCR5*, *PDCD1* (PD1), *ICOS*, and *BCL6* expression. Cells from the T15 cluster expressed transcripts indicative of mucosal-associated invariant T (MAIT) cells (28), including *ZBTB16* and *TRA1V-2*. We next compared the numbers of cells from each of the T lymphocyte clusters derived from healthy individuals and patients with UC (Fig. 4C). In the peripheral blood, cluster T8 cells were enriched in patients with UC, raising the possibility of previously unrecognized $\gamma\delta$

T cell states or subsets that may be more abundant in the setting of disease. In the intestine, the T7 (T_{reg}), T5 (T_{FH}), and T10 (CD8⁺ T_{RM}) cell clusters were enriched in patients with UC.

Because T_{reg} cells are known to prevent inflammation and autoimmunity (26), it might have been predicted that T_{reg} cells would be numerically reduced in patients with UC. However, we observed an enrichment of the T7 T_{reg} cell cluster in patients with UC (Fig. 4C), consistent with previously published reports (8, 9), suggesting that inflammation was not due to insufficient numbers of T_{reg} cells. Rather, we hypothesized that this finding might reflect an expansion of T_{reg} cells to control ongoing inflammation. We further reasoned that T_{reg} cells from patients with UC might express transcripts leading to defective T_{reg} cell function that could contribute to disease development despite increased numbers of these cells. Comparison of the gene expression profiles of T_{reg} cells from healthy individuals and patients with UC revealed 288 differentially expressed genes (Fig. 4D and table S5), some of which have previously been reported to play a role in T_{reg} cell function, suggesting that the current approach was capable of identifying functionally important genes. For example, expression of *SATB1*, repression of which is necessary for T_{reg} cell suppressive function (29, 30), was increased in T_{reg} cells from patients with UC; conversely, *KLF2*, *MYC*, and *ITGB1* expression was reduced in T_{reg} cells from patients with UC, consistent with previously published work demonstrating a role of these factors in T_{reg} cell function (31–33). However, most of the genes differentially expressed between T_{reg} cells from healthy individuals versus patients with UC had not been previously linked to T_{reg} cell function. As a first step toward demonstrating that genes identified by these analyses might indeed represent previously unrecognized regulators of T_{reg} cell function, we selected one such gene, *ZEB2*, which has been previously shown to promote effector function in murine CD8⁺ T cells (34, 35), for further studies. The observation that *ZEB2* was more highly expressed in T_{reg} cells derived from patients with UC raised the possibility that down-regulation of *ZEB2* may be required for optimal T_{reg} cell function. To test this possibility, we transduced in vitro-induced murine T_{reg} cells with a short hairpin RNA (shRNA) construct targeting Zeb2. T_{reg} cells transduced with a Zeb2 shRNA construct exhibited enhanced suppressive function compared with control T_{reg} cells transduced with a nontargeting shRNA construct (Fig. 4E). To confirm these results, we treated *ER^{Wt}Zeb2^{f/f}* and *ER^{Cre}Zeb2^{f/f}* mice with tamoxifen to induce Zeb2 deletion, FACS-purified naïve CD4⁺CD25⁻ T cells, and cultured these cells in T_{reg} cell-inducing cytokine conditions. Control and Zeb2-deficient T_{reg} cells were then FACS-purified and tested in an in vitro suppression assay; we observed that Zeb2-deficient T_{reg} cells exhibited enhanced suppressive function compared with control T_{reg} cells (Fig. 4F and fig. S5).

Differential enrichment of heterogeneous $\gamma\delta$ T cell clusters in health versus UC

The aforementioned analyses (Fig. 4C) raised the possibility that distinct $\gamma\delta$ T cell states or subsets might be differentially enriched in the setting of health versus UC. To begin to understand the differences among these putative $\gamma\delta$ T cell states, we performed differential gene expression analyses of the three $\gamma\delta$ T cell clusters (T8, T13, and T16) that we defined. These analyses revealed a number of genes that were differentially expressed among the three $\gamma\delta$ T cell clusters (Fig. 5, A and B, and table S6). For example, T8 cluster cells expressed high levels of *CCR7*; T13 cells expressed high levels of *KLRB1*

**Fig. 4.** $CD4^+$ T_{reg} cells from patients with UC and healthy individuals exhibit distinct transcriptional signatures.

(A) Phenotypic annotations of T lymphocyte clusters. (B) t-SNE plots of T lymphocyte clusters, colored by cluster identity (upper left), anatomic location from which cells were derived (upper right), and health status (lower left). (C) Quantitation of T lymphocyte clusters that were enriched or depleted in health versus UC, expressed as absolute numbers. (D) Mean expression of selected genes that were differentially expressed between T7 cluster $CD4^+$ T_{reg} cells derived from healthy individuals (blue) versus patients with UC (red); see also table S5. UMI, unique molecular identifier. (E) In vitro suppression assay using induced T_{reg} cells transduced with nontargeting (NT) shRNA ($n = 3$) or Zeb2 shRNA ($n = 3$) or (F) induced T_{reg} cells from tamoxifen-treated $ER^{Wt}Zeb2^{fl/fl}$ ($n = 3$) and $ER^{Cre}Zeb2^{fl/fl}$ ($n = 3$) mice. Putative T_{reg} cells were sorted on the basis of high CD4 and CD25 expression, and these cells expressed high levels of Foxp3; see also fig. S5. Error bars indicate SEM. Two-sided Wilcoxon rank sum test (C); unpaired Student's *t* test for each T_{conv} : T_{reg} ratio (E and F). T_{conv} , conventional T cell ($CD4^+ CD25^-$). * $P < 0.05$, ** $P < 0.01$, and *** $P < 0.001$.

(CD161) and *S100B*; and T16 cells expressed high levels of *KLRC1* (NKG2A), *GNLY*, and *XCL1*. To confirm whether these $\gamma\delta$ T cell states could be discerned in human peripheral blood, we constructed a panel of 35 protein markers based on differentially expressed genes among T8, T13, and T16 cluster cells derived from our scRNA-seq analyses. We then performed mass cytometry using peripheral blood from an independent cohort of healthy individuals and patients with UC (fig. S6 and table S7). In addition to unbiased analysis of the dataset using PhenoGraph (fig. S6), targeted analysis of $\gamma\delta$ T cells was performed. $\gamma\delta$ T cells were electronically gated on the basis of $CD45^+ CD3^+ \gamma\delta TCR^+$ positivity and then subjected to UMAP analysis, revealing three clusters of $\gamma\delta$ T cells (Fig. 5C).

The UMAP analyses suggested that the combination of 35 protein markers together could distinguish these putative $\gamma\delta$ T cell states. We next asked whether these putative $\gamma\delta$ T cell states could be discerned using only a few protein markers selected from our differential gene expression analyses. $\gamma\delta$ T cells were electronically gated on the basis of $CD45^+ CD3^+ \gamma\delta TCR^+$ positivity, and expression of *CCR7*, *CD161*, and *NKG2A* was analyzed. Putative T13 cluster cells could be distinguished from T8 and T16 cluster cells on the basis of high NKG2A expression (Fig. 5D). Putative T8 and T16 cluster cells, both of which expressed low levels of NKG2A, could be distinguished on the basis of *CCR7* and *CD161* protein expression, with T8 cluster cells tending to express higher levels of *CCR7* and T16 cluster cells expressing higher levels of *CD161*. Last, we observed that, as predicted by our scRNA-seq analyses (Fig. 4C), putative T8 cluster cells represented a higher proportion of $\gamma\delta$ T cells in the peripheral blood of patients with UC compared with healthy individuals (Fig. 5D).

Clonal expansion of a UC-associated $CD8^+ T_{RM}$ cell cluster with enhanced inflammatory properties

As described above, we annotated four putative $CD8^+ T_{RM}$ -like cell clusters (T1, T2, T10, and T14) and hypothesized that these clusters might represent states between which T_{RM} cells transit differentially during health and disease. To

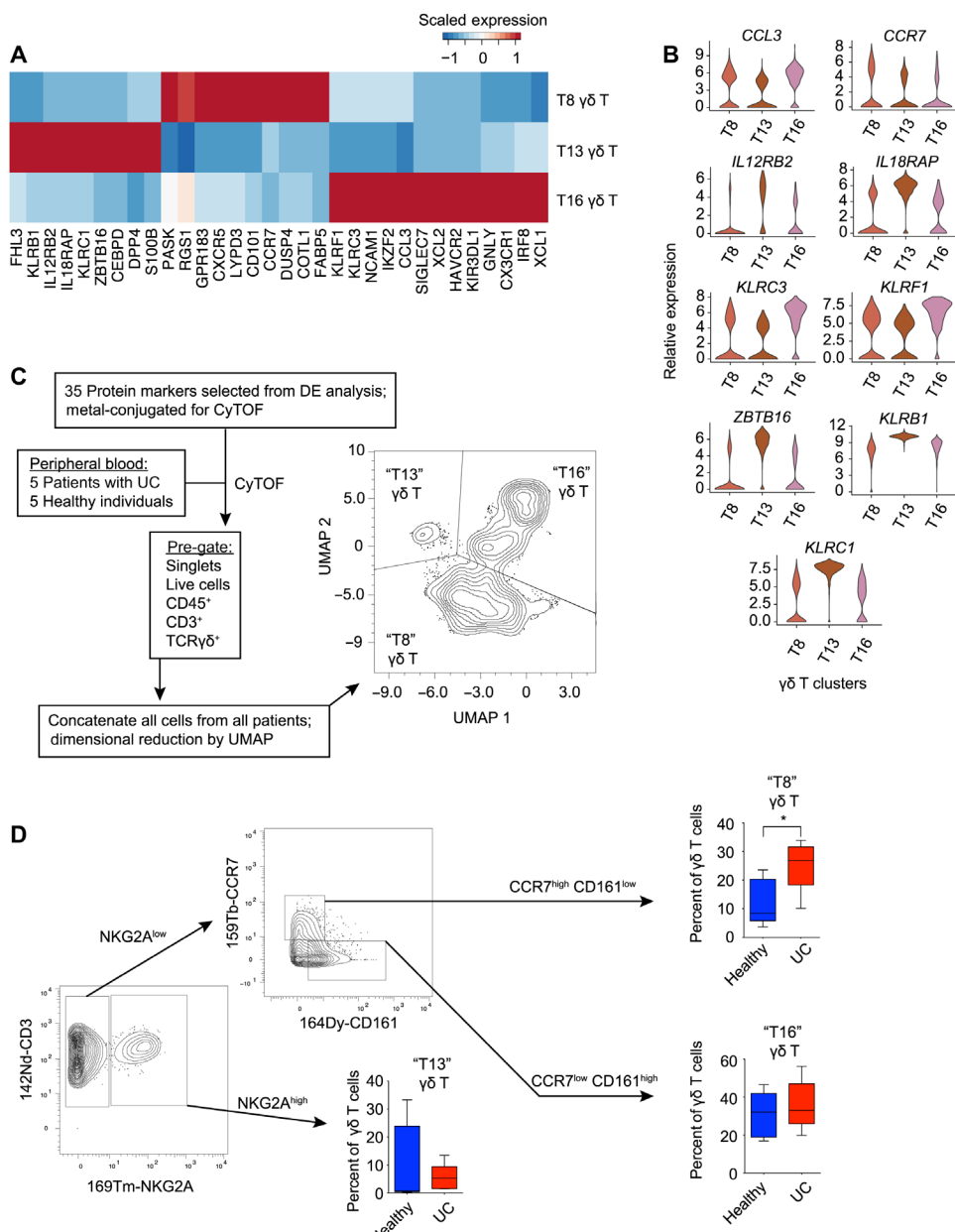


Fig. 5. Differential enrichment of $\gamma\delta$ T cell clusters in health versus UC. (A) Heatmap of mean expression of selected genes differentially expressed between $\gamma\delta$ T cell clusters (T8, T13, and T16). (B) Violin plots of selected genes differentially expressed by $\gamma\delta$ T cell clusters (T8, T13, and T16). (C) Overview of the design for mass cytometry (CyTOF) analysis of peripheral blood from healthy individuals ($n=5$) and patients with UC ($n=5$), with UMAP analysis of $\gamma\delta$ T cells from all patients. DE, differential gene expression. (D) Gating strategy to identify $CCR7^{high} CD161^{low}$ $NKG2A^{low}$ ("T8"), $NKG2A^{high}$ ("T13"), and $CCR7^{low} CD161^{high}$ $NKG2A^{low}$ ("T16") clusters, with the proportion of each cell cluster represented among all $\gamma\delta$ T cells for each participant, calculated separately for healthy individuals versus patients with UC. Error bars indicate SEM. Unpaired Student's *t* test (D). **P* < 0.05.

investigate this possibility, we looked for evidence of TCR clonotypes shared among the T cell clusters we previously defined. In healthy individuals, clonotypes were shared across cells from the CD8⁺ T_{RM} T1, T2, and T14 clusters (Fig. 6A and fig. S3B); by contrast, in patients with UC, clonotypes were shared among the CD8⁺ T_{RM} T1, T2, and T10 cell clusters (Fig. 6B and fig. S3B). In line with these observations, there was increased clonal expansion of cells from the

T1 and T14 clusters preferentially in healthy individuals; conversely, there was increased clonal expansion of cells from the T10 cluster in patients with UC (Fig. 6C). Moreover, we observed that in the setting of UC, there was a marked increase in clonotypes shared between the T10 and T8 clusters; because T10 cluster cells were derived predominantly from intestinal tissue whereas T8 cluster cells were almost exclusively derived from peripheral blood (fig. S4D), these results indicated trafficking of clonally related cells between the two compartments. We detected a significantly greater proportion of clonally related T10 and T8 cluster cells in patients with UC compared with healthy individuals (Fig. 6D). Moreover, for certain clonotypes, the number of cells in the tissue (T10) was greater than that in the blood (T8), whereas for other clonotypes, the number of cells in the blood was greater than that for tissue (Fig. 6E). Differential expression analyses revealed changes in genes encoding trafficking molecules (23), including decreased expression of CD69 and CRTAM and increased expression of SELL, KLF2, and S1PR1 in blood T8 cells compared with clonally related tissue T10 cells (Fig. 6, F and G). Together, these results indicate that in the setting of UC, clonally related CD8⁺ T cells may modulate their gene expression to enable trafficking between blood and intestinal tissue.

These findings also suggested a spectrum of states between which clonally related CD8⁺ T_{RM} cells transit differentially in health versus UC. To begin to understand the differences between these putative CD8⁺ T_{RM} cell states, we performed differential gene expression and pathway analyses of the four T_{RM} cell clusters (T1, T2, T10, and T14) (Fig. 7, A and B, and table S8). These analyses revealed 481 genes differentially expressed between T10 cluster cells and cells from the other three CD8⁺ T_{RM} clusters. These included increased expression of transcripts encoding inflammatory mole-

cules and cytolytic granules, such as perforin and granzymes A, B, H, K, and M; metabolic regulators such as FABP5, which has been shown to support T_{RM} cell differentiation (36); and a number of key transcription factors, including ZEB2 (34, 35) and Eomes (37), both of which have previously been implicated in circulating effector and memory CD8⁺ T cell differentiation (38). Because Eomes has been previously shown to promote its own expression (39), we hypothesized

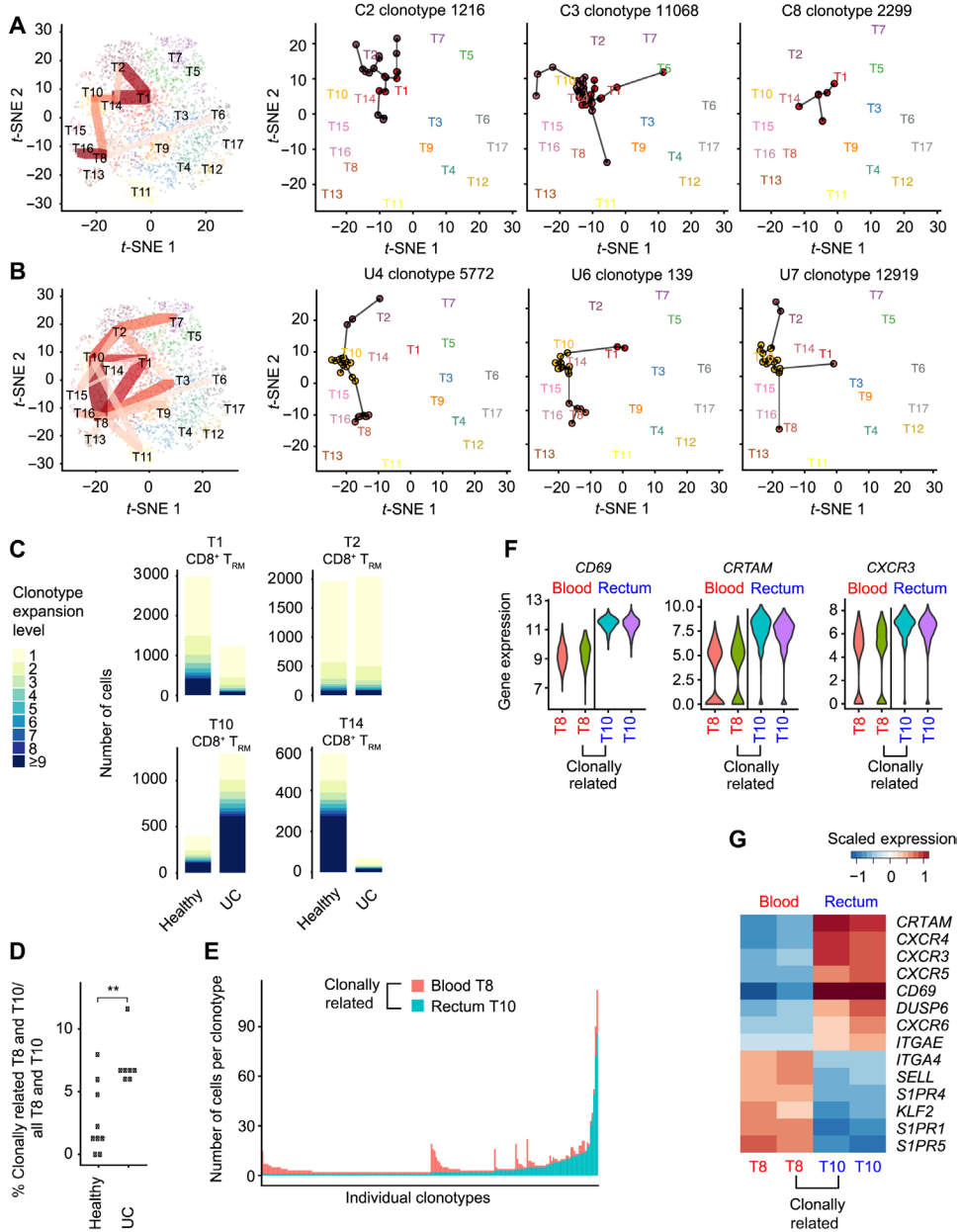


Fig. 6. Clonally expanded cells from a CD8⁺ T_{RM} cluster enriched in patients with UC. t-SNE plots of T cell clusters of healthy individuals (A) and patients with UC (B), colored by cluster identity. For summary plots (left plots), red lines indicate TCR clonotypes shared among clusters and line weight represents number of shared clonotypes; three selected clonotypes from three representative healthy individuals (A; right three plots) or patients with UC (B; right three plots) are shown as examples. (C) Comparison of clonotypic expansion exhibited by cells from CD8⁺ T_{RM} cell clusters (T1, T2, T10, and T14) from healthy individuals and patients with UC. (D) Quantitation of clonally related T8 and T10 cells in healthy controls and patients with UC, represented as proportion of clonally related T8 and T10 cells among all T8 and T10 cells in each individual. (E) Anatomic origin of clonally related blood T8 and rectal T10 cells. Each column represents a single clonotype and is colored on the basis of anatomic location (rectum, blue; peripheral blood, red); numbers of clonally related cells derived from each location are indicated on the y axis. (F and G) Violin plots (F) and heatmap (G) of selected differentially expressed genes in clonally related and clonally unrelated T8 and T10 cells (peripheral blood, red; rectum, blue). Two-sided Wilcoxon rank sum test (D). **P < 0.01.

that Eomes might be a critical regulator of the T10 CD8⁺ T_{RM} transcriptional program.

Applying *in situ* RNA hybridization using *EOMES* as a marker of T10 CD8⁺ T_{RM} cells, we first asked whether these cells could be

detected in intestinal tissue specimens from an independent cohort of UC patients with active disease. We performed pairwise comparisons between affected and unaffected tissue derived from the same patients with UC and observed that T10-like cells were increased in affected compared with unaffected tissue in this cohort (Fig. 7, C to E). Next, we investigated whether CD8⁺ T cells might play a role in mediating intestinal inflammation using an established interleukin-10 (IL-10)-deficient piroxicam-induced enterocolitis mouse model (40). We observed a significant increase in colonic CD8⁺ T cells in IL-10-deficient mice that were fed piroxicam-containing chow compared with control mice that were fed control chow (fig. S7A). To test whether depletion of CD8⁺ T cells might ameliorate disease, we treated IL-10-deficient mice that were fed piroxicam-containing chow with either depleting anti-CD8α or isotype control antibodies and their weight monitored daily over 2 weeks. Treatment with anti-CD8α antibodies resulted in a substantial depletion of CD8⁺ T cells in the peripheral blood and colonic tissue (fig. S7B). Moreover, compared with treatment with isotype control antibodies, treatment with anti-CD8α antibodies resulted in a reduction of weight loss and colonic pathology induced by piroxicam (Fig. 8A and fig. S7C), suggesting a role for CD8⁺ T cells in the piroxicam-induced IL-10-deficient mouse model, consistent with prior reports (40, 41), although it remains possible that CD8α⁺ dendritic cells and/or CD8αα⁺ γδ T cells may also play a contributing role in this model. To determine whether ectopic expression of Eomes in CD8⁺ T cells could influence disease severity in a model of intestinal inflammation, we adoptively transferred CD8⁺ T cells transduced with control or Eomes retroviral constructs into recombination-activating gene 1 (RAG1)-deficient mice before challenging them with dextran sulfate sodium (DSS). We observed that mice receiving CD8⁺ T cells transduced with the Eomes construct lost significantly more weight and exhibited more colonic pathology than mice that received CD8⁺ T cells transduced with the control construct (Fig. 8B and fig. S7D), suggesting that ectopic Eomes expression is sufficient to confer CD8⁺ T cells with enhanced pathogenic properties.

We next investigated what gene targets Eomes might be acting upon to mediate these effects. Putative gene targets of Eomes have

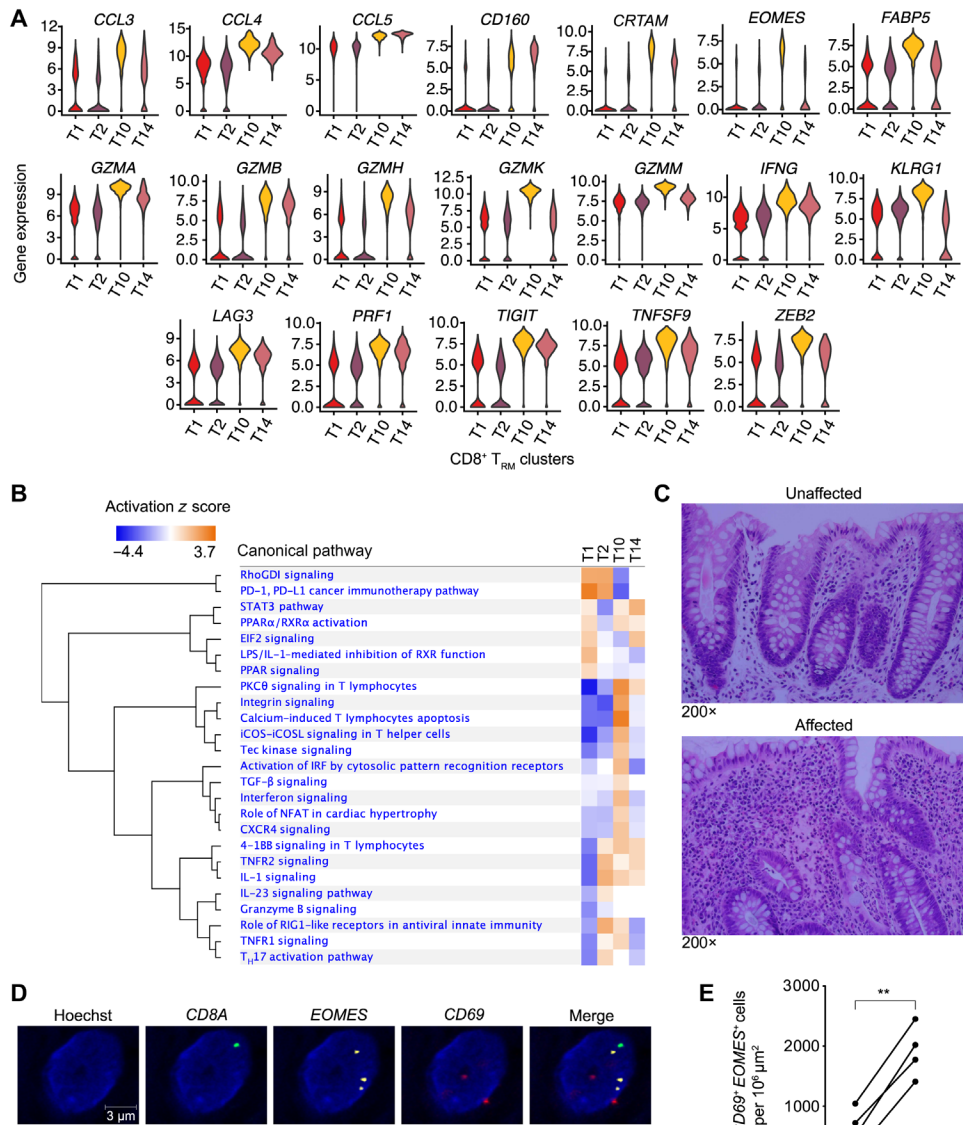


Fig. 7. Cells from a CD8⁺ T_{RM} cell cluster with enhanced inflammatory properties are increased in affected colonic tissue from patients with UC. (A) Violin plots of selected genes differentially expressed by the four CD8⁺ T_{RM} cell clusters (T1, T2, T10, and T14). (B) Pathway analysis of genes differentially expressed by the T10 CD8⁺ T_{RM} cluster compared with all other CD8⁺ T_{RM} clusters. (C) Representative hematoxylin and eosin-stained images of unaffected and affected colonic tissue from a patient with UC used for RNA in situ hybridization (ISH) analyses shown in (D) and (E). Representative ISH images of affected colonic tissue (D) and quantitation of CD8⁺CD69⁺EOMES⁺ cells from unaffected and affected regions of colonic tissue from patients with UC ($n = 5$) (E). Paired Student's *t* test (E). ** $P < 0.01$.

been previously identified in thymic innate memory CD8⁺ T cells (42) and in vitro-differentiated CD8⁺ T cells (39) using chromatin immunoprecipitation sequencing approaches, but such approaches are not feasible in intestinal CD8⁺ T_{RM} cells because of technical challenges with cell numbers. Moreover, the low numbers of intestinal CD8⁺ T cells that can be recovered in commonly used intestinal inflammation models precluded their use as a model system with which to identify Eomes gene targets in intestinal CD8⁺ T_{RM} cells.

Thus, to identify putative gene targets of Eomes specifically in intestinal CD8⁺ T_{RM} cells, we applied the assay for transposase-accessible chromatin using sequencing (ATAC-seq) in the context of the lymphocytic choriomeningitis virus (LCMV) model system in which intestinal CD8⁺ T_{RM} cells have been widely studied (43). P14 CD8⁺CD45.1⁺ T cells, which have transgenic expression of a TCR that recognizes an immunodominant epitope of LCMV, were adoptively transferred into congenic CD45.2⁺ wild-type recipient mice subsequently infected with LCMV 1 day later. Donor CD45.1⁺ P14 T cells were FACS-sorted from the small intestine epithelial lymphocyte compartment of recipient mice at 7 and 30 days after infection and processed for ATAC-seq. We searched for predicted Eomes binding motifs in accessible enhancer and promoter regions and looked for overlap of these genes with the T10 CD8⁺ T_{RM} cluster transcriptional signature. These analyses confirmed known Eomes gene targets such as *Ifng* and *Gzma* (37) but identified other molecules, such as *Klrg1*, a killer lectin receptor, and *Icos*, a costimulatory molecule, as putative Eomes gene targets (Fig. 8C and table S9). To test whether ectopic expression of Eomes resulted in increased expression of putative gene targets that we identified by ATAC-seq analysis, we transduced congenically distinct CD8⁺ T cells with control (CD45.1) or Eomes (CD45.1.2) retroviral constructs before adoptive transfer into recipient mice (CD45.2) subsequently infected with LCMV and used flow cytometry to examine the protein expression of several putative targets in intestinal CD8⁺ T cells at 7 days after infection. Compared with intestinal CD8⁺ T cells expressing control constructs, intestinal CD8⁺ T cells expressing Eomes constructs expressed higher levels of interferon- γ (IFN γ), granzyme A, and KLRG1 protein and lower levels of inducible T cell costimulator (ICOS) protein (Fig. 8D). Together, these findings suggest the possibility that in UC, up-regulation of key factors such as Eomes in intestinal CD8⁺ T_{RM} cells may promote their conversion into a pathogenic state exhibiting enhanced inflammatory and cytolytic properties.

DISCUSSION

Recent studies have begun to apply single-cell transcriptomic approaches to investigate the mechanisms underlying the complex

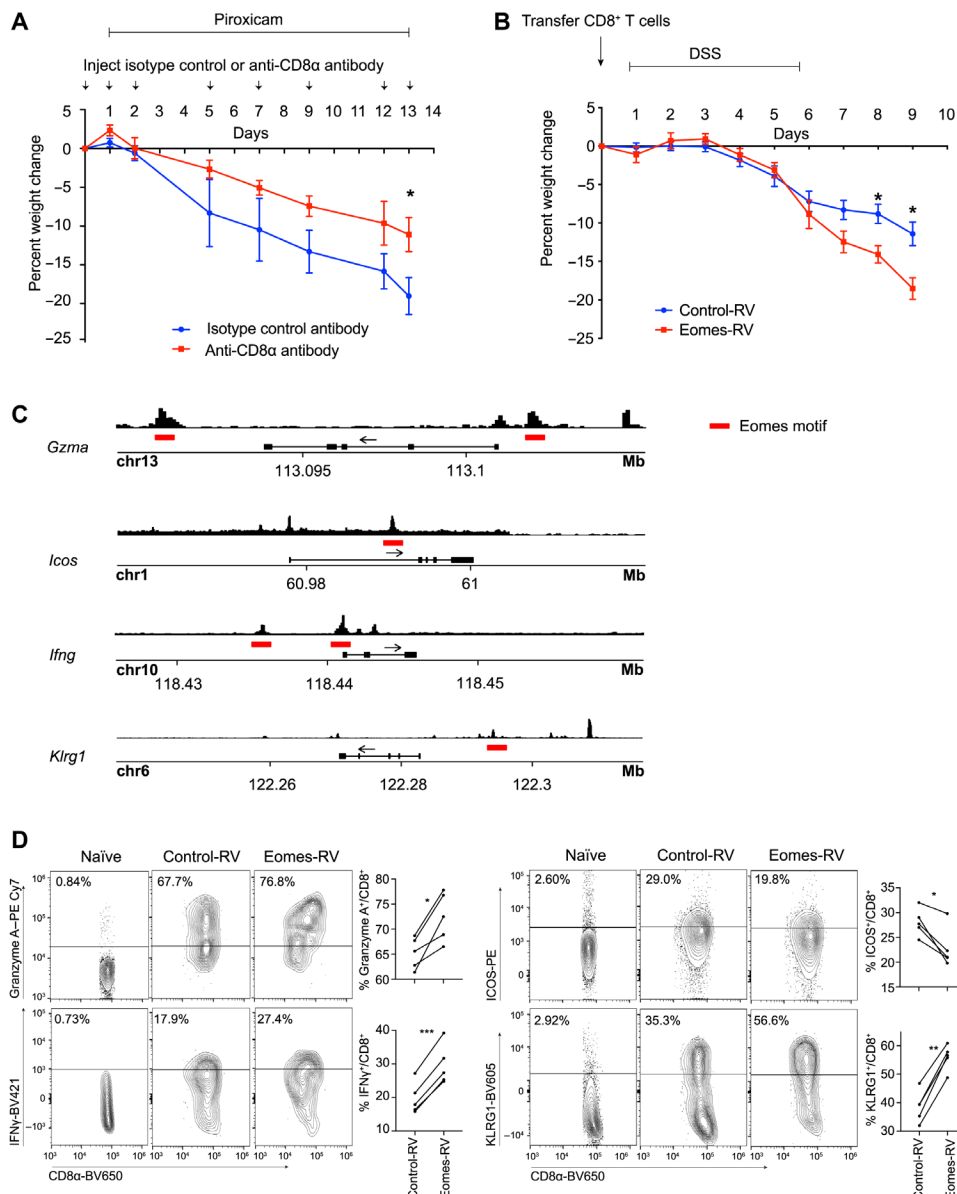


Fig. 8. Eomes may regulate the T10 CD8 $^+$ TRM cluster transcriptional program. **(A)** Percent weight change observed with CD8 α depletion ($n = 5$) versus isotype control ($n = 5$) in an IL-10-deficient piroxicam-induced enterocolitis mouse model, expressed as percent of weight at the start of the experiment. Error bars indicate SEM. Data are representative of two independent experiments. **(B)** Percent weight change observed in RAG1-deficient mice receiving 5×10^5 FACS-sorted, green fluorescent protein-positive control-retrovirus (RV) ($n = 13$) or Eomes-RV ($n = 8$) CD8 $^+$ T cells and treated with DSS, expressed as percent of weight at the start of the experiment. Error bars indicate SEM. Data are representative of two independent experiments. **(C)** ATAC-seq tracks with putative Eomes motifs (indicated with red lines) near accessible promoter regions for selected genes are shown. P14 CD8 $^+$ T cells were adoptively transferred into congenic recipients subsequently infected with LCMV Armstrong; cells were FACS-sorted at days 7 and 30 after infection (two technical replicates per time point) and subjected to ATAC-seq. Representative day 7 post-infection ATAC-seq tracks are shown. **(D)** P14 CD8 $^+$ T cells were transduced with control-RV (CD45.1) or Eomes-RV (CD45.1.2) constructs and adoptively transferred into congenic recipients (CD45.1.2) subsequently infected with LCMV Armstrong ($n = 5$). Expression of selected proteins by control-RV– versus Eomes-RV-expressing CD8 $^+$ T cells was analyzed by FACS at 7 days after infection; staining of naïve CD8 $^+$ T cells from an uninfected mouse are shown as a control. Data are representative of two independent experiments. PE, R-phycocerythrin; PE-Cy7, R-phycocerythrin-cyanine7 tandem fluorochrome; BV421, Brilliant Violet 421; BV605, Brilliant Violet 605. Unpaired Student's *t* test (A and B) or paired Student's *t* test (D). **P* < 0.05, ***P* < 0.01, and ****P* < 0.001.

dysregulation of the immune system in IBD (18, 19). Our integrated single-cell transcriptomic and antigen receptor sequencing analyses have resulted in several insights into the immunobiology of UC. First, we annotated multiple clusters of plasma cells in intestinal tissue and observed that BCR clonotypes were shared among cells from many of these clusters, raising the possibility that plasma cells may transit among a spectrum of states. Plasma cells from patients with UC exhibited a marked shift toward a specific IgG $^+$ cluster (B1), in contrast to plasma cells from healthy individuals, which were predominantly IgA $^+$, in accordance with early immunohistochemical findings first reported in the 1970s (44) and confirmed in subsequent studies (45–47). It has been shown that colitogenic intestinal bacteria can be coated by high levels of IgA (48), suggesting that the ability of healthy individuals to produce IgA in the gut microenvironment may enable them to control specific inflammatory commensals that might otherwise initiate intestinal inflammation. Alternatively or in addition, IgG antibodies may themselves be pathogenic because it was previously proposed that an increase in anticommensal IgG antibodies in patients with UC may lead to inflammation through IgG-mediated Fc γ R receptor activation and type 17 immunity (45).

Second, we envision that the current dataset can be used as a starting point to identify genes previously unknown to be dysregulated in IBD in an immune cell type-specific manner for further investigation. As an example, we observed an enrichment of T_{reg} cells (contained within cluster T7) in patients with UC, raising the possibility that these cells might be functionally impaired despite being present in adequate numbers. Further analyses revealed a number of transcripts that were differentially expressed between T_{reg} cells derived from healthy individuals compared with those from patients with UC, many of which were not previously known to have a role in T_{reg} cells. We selected ZEB2 for further study, which, owing to its observed up-regulation in T_{reg} cells from patients with UC, was hypothesized to impair T_{reg} cell function; knockdown or deletion of Zeb2 resulted in enhanced murine T_{reg} cell suppressive activity. This

finding, together with the observations that the expression of several previously known regulators of murine T_{reg} cells was also altered in T_{reg} cells from patients with UC, suggests the potential value of the dataset in selecting putative regulators of healthy versus disease T_{reg} cell states for further study.

A third insight that derives from these analyses is the finding of heterogeneity among CD8⁺ T_{RM} cells in the human intestine. T_{RM} cells are a subset of memory T lymphocytes that reside within tissues and provide essential protection at body surfaces (23), but to date, there has been only limited evidence for heterogeneity among murine (49, 50) and human T_{RM} cells (51). T_{RM} cells have been implicated in human autoimmune diseases such as vitiligo and psoriasis (52, 53), and recent studies have suggested a role for CD4⁺ T_{RM} cells (24, 25) in IBD. We detected four transcriptionally distinct clusters of CD8⁺ T_{RM} cells, one of which (T10) contained cells that had undergone significant clonal expansion predominantly in patients with UC. The finding that TCR clonotypes were shared among cells from the four CD8⁺ T_{RM} cell clusters supports the hypothesis that these clusters represent states between which CD8⁺ T_{RM} cells transit; in the setting of UC, we observed a marked shift of cells toward the putative T10 differentiation state. Moreover, the observation that increased numbers of cells in the peripheral blood that were clonally related to T10 CD8⁺ T_{RM} cells in the intestine were increased in UC is intriguing in light of recent reports that murine and human T_{RM} cells can exit the tissue and recirculate (54, 55). Together, our data suggest a role for CD8⁺ T_{RM} cells in UC and raise the possibility that during IBD exacerbations, CD8⁺ T_{RM} cells may exit the intestinal tissue and recirculate, providing a potential explanation for the tendency for IBD to affect multiple organ systems outside of the gastrointestinal tract.

Compared with cells in the other T_{RM} states, cells in the T10 differentiation state expressed higher levels of genes encoding molecules that confer inflammatory and effector properties, such as cytokines, cytolytic granules, and killer lectin receptors. Our analyses nominate the T-box transcription factor Eomes as a regulator of the putative T10 CD8⁺ T_{RM} cell transcriptional state. Eomes and T-bet are highly homologous members of the T-box family of transcription factors and are highly expressed by activated CD8⁺ T cells and resting and activated NK cells (37). Eomes and T-bet have cooperative functions (56) in inducing effector functions and enhanced expression of CD122, the receptor controlling IL-15 responsiveness, which underlies proliferative renewal after clearance of microbial pathogen (57, 58). Eomes also has functions that are distinct from those of T-bet, such as promoting self-renewal of long-lived memory cells (59), and has been shown to be up-regulated in CD8⁺ T cells during chronic infection (60). In the context of murine skin T_{RM} cell differentiation in response to microbial infection, both Eomes and T-bet undergo initial up-regulation but are subsequently down-regulated to enable responsiveness to transforming growth factor-β signaling and continued T_{RM} cell differentiation (61). Eomes is extinguished by 2 to 4 weeks after infection, at least in skin T_{RM} cells, but low levels of T-bet are necessary for the maintenance of CD122 and survival of T_{RM} cells (61–63); it is therefore intriguing that cells in the putative T10 CD8⁺ T_{RM} transcriptional state expressed high levels of Eomes. This T10 CD8⁺ T_{RM} cluster, which exhibited high expression of transcription factors such as *EOMES*, appears to be transcriptionally distinct from a previously described CD8⁺IL17A⁺ T cell cluster (19), which expressed high levels of *RORA* and *RORC*, identified by scRNA-seq; moreover, it remains

unknown how the T10 CD8⁺ T_{RM} cluster described here relates to a CD3⁺CD4⁻CD8⁻IL-17A⁺ T cell cluster recently identified using mass cytometry (9). Future work will further investigate the degree of heterogeneity among intestinal CD8⁺ T cells with respect to function and plasticity in health and IBD.

Our data suggest a model in which T_{RM} cells exist in equilibrium across several differentiation states in the healthy condition. In the setting of UC, T_{RM} cells may up-regulate Eomes, which binds to a number of downstream gene targets. On the basis of our ATAC-seq analyses in murine intestinal CD8⁺ T cells, putative gene targets may include inflammatory cytokines (*Ifng*), cytolytic granules (*Gzma*), chemokines (*Ccl3*, *Ccl4*, and *Ccl5*), molecules that promote survival (*Bach2*, *Cd27*, and *Il2rb*), killer cell lectin receptors (*Klrb1*, *Klrc1*, *Klrd1*, *Klrg1*, and *Krk1*), costimulatory molecules [*Tnfrsf18* (GITR), *Tnfrsf4* (OX40R), and *Icos*], and trafficking molecules such as *Crtam* (64). A caveat of the current study is the use of an infection system, owing to technical limitations with experimental colitis models, with which to identify putative Eomes gene targets in intestinal CD8⁺ T_{RM} cells. Nonetheless, it appears that up-regulation of Eomes in CD8⁺ T_{RM} cells, through its actions on a diverse set of gene targets, may promote the acquisition of an inflammatory and pathogenic T_{RM} cell transcriptional program.

Overall, our work has resulted in an integrated single-cell transcriptomic and antigen receptor sequencing dataset that expands the single-cell data available in human IBD. The study identifies alterations in immune cell types and clonal relationships that occur in the context of disease, including plasma cells, T_{reg} cells, γδ T cells, and CD8⁺ T_{RM} cells, and will enable other investigators to identify additional UC-associated changes in a cell type- and tissue-specific manner for further study. This is likely to accelerate mechanistic and functional investigations into the role of specific genes in relevant immune cell types and states in UC.

MATERIALS AND METHODS

Study design

The purpose of this study was to gain a broader understanding of the heterogeneity and clonal relationships of adaptive immune cells in the context of human UC. To this end, we generated and analyzed scRNA and antigen receptor sequencing data generated from human peripheral blood and gastrointestinal mucosal tissue samples.

Human participants

The Human Research Protection Programs at the University of California, San Diego (UCSD) and the VA San Diego Healthcare System approved the study. Intestinal biopsies and peripheral blood were obtained from patients undergoing colonoscopy at the UCSD and the VA San Diego Healthcare System after obtaining informed consent. Healthy individuals were undergoing colonoscopy as part of routine clinical care for colorectal cancer screening/surveillance or noninflammatory gastrointestinal symptoms that included constipation or rectal bleeding. Inclusion criteria included age over 18 years old and absence of significant comorbidities or colorectal cancer. UC patients with active endoscopic disease were selected. Details of the study participants are provided in table S2.

Human peripheral blood mononuclear cell isolation

Blood was collected in a BD Vacutainer CPT tube and centrifuged at 400g for 25 min. The buffy coat layer was removed, washed, and

counted. Cells were resuspended in freezing buffer {10% (v/v) dimethyl sulfoxide (DMSO; Sigma-Aldrich), 40% (v/v) complete RPMI [RPMI (Corning) + 10% (v/v) fetal bovine serum (FBS; Life Technologies) + penicillin (100 U/ml)/streptomycin (100 µg/ml) (Life Technologies)], and 50% (v/v) FBS}, placed into a freezing container (Mr. Frosty), and stored at -80°C. Cells were recovered, washed, filtered, and used for mass cytometry [cytometry by time of flight (CyTOF, Fluidigm)] as described below or labeled with anti-human CD45 (2D1) (BioLegend) for sorting. CD45⁺ immune cells were sorted on a FACSAria II (BD Biosciences) using gating strategy shown in fig. S1A.

Human intestinal cell isolation

Intestinal biopsies were obtained with endoscopic biopsy forceps from the rectum and collected in a conical tube with Hanks' balanced salt solution (HBSS; Corning). Intestinal biopsies were transferred into freezing buffer [10% (v/v) DMSO, 40% (v/v) complete RPMI, and 50% (v/v) FBS] and stored at -80°C. Biopsies were recovered, incubated in HBSS on a shaker, then incubated twice in HBSS and 5 mM dithiothreitol (Thermo Fisher Scientific) with shaking, and then washed in HBSS. Intestinal biopsies were mechanically dissociated, then placed into 10 ml of digestion mixture [complete RPMI, collagenase type VIII (1.5 mg/ml) (Sigma-Aldrich), and deoxyribonuclease I (50 µg/ml) (Roche)] on a rocker at 37°C for 20 min, filtered, and stained with anti-human CD45. CD45⁺ immune cells were sorted on a FACSAria II using the gating strategy shown in fig. S1A.

10x Genomics library preparation and sequencing

Cells were washed and resuspended in phosphate-buffered saline and 0.04% (w/v) bovine serum albumin per the manufacturer's guidelines. Single-cell libraries were prepared according to the protocol for 10x Genomics for Single Cell V(D)J and 5' Gene Expression. About 20,000 sorted CD45⁺ cells were loaded and partitioned into Gel Bead In-Emulsions. scRNA libraries were sequenced on a HiSeq 4000 (Illumina). The BCR and TCR libraries were amplified according to the manufacturer's protocol and sequenced on a NovaSeq S4 (Illumina).

Mice

All mice were housed under specific pathogen-free conditions in an American Association of Laboratory Animal Care-approved facility at UCSD, and all procedures were approved by the UCSD Institutional Animal Care and Use Committee. C57BL/6 CD45.1, CD45.2, CD45.1.2, P14 TCR transgenic (CD45.1 or CD45.1.2, both maintained on a C57BL/6 background), RAG1-deficient, and IL-10-deficient mice were bred at UCSD or purchased from the Jackson Laboratories. Mice with a loxP-flanked Zeb2 allele (35, 65) were bred with Rosa26Cre-ERT2 (ERCre) mice (66) and were maintained on a C57BL/J6 background. Rosa26Cre-ERT2-mediated deletion of the floxed Zeb2 gene was induced by oral gavage of 1 mg of tamoxifen (Cayman Chemical Company) emulsified in 100 µl of sunflower seed oil (Sigma-Aldrich) for five consecutive days and then rested for 5 days. Cells for T_{reg} cell suppression assays were obtained from male mice that were 12 to 28 weeks old.

SUPPLEMENTARY MATERIALS

immunology.science.org/cgi/content/full/5/50/eabb4432/DC1
Materials and Methods

Fig. S1. Overview of experimental design, quality control metrics of single-cell sequencing data, and assessment of overall antigen receptor diversity in healthy individuals and patients with UC.

Fig. S2. scRNA-seq reveals heterogeneous B lymphocyte clusters.

Fig. S3. Analyses of clonal relationships in health and UC.

Fig. S4. scRNA-seq reveals heterogeneous T lymphocyte clusters.

Fig. S5. Analysis of Zeb2 knockdown or Zeb2-deficient T_{reg} cells.

Fig. S6. Mass cytometry analysis of peripheral blood.

Fig. S7. CD8⁺ T cell analysis and histopathology in mouse models of intestinal inflammation.

Table S1. Raw data file.

Table S2. Demographics for patient samples.

Table S3. Quality control metrics for single-cell sequencing data.

Table S4. Differential gene expression analyses of plasma cell clusters.

Table S5. Differential gene expression analyses between γδ T cell clusters T8, T13, and T16.

Table S6. Differential gene expression analyses between T7 cluster cells from patients with UC versus healthy individuals.

Table S7. Metal-conjugated antibodies for mass cytometry.

Table S8. Differential gene expression analyses of CD8⁺ tissue-resident memory cell clusters.

Table S9. Putative Eomes gene targets in intestinal CD8⁺ T cells.

References (67–75)

[View/request a protocol for this paper from Bio-protocol.](https://doi.org/10.1126/sciimmuno.5.eabb4432)

REFERENCES AND NOTES

- B. Khor, A. Gardet, R. J. Xavier, Genetics and pathogenesis of inflammatory bowel disease. *Nature* **474**, 307–317 (2011).
- C. Abraham, J. H. Cho, Inflammatory bowel disease. *N. Engl. J. Med.* **361**, 2066–2078 (2009).
- N. Kamada, T. Hisamatsu, S. Okamoto, H. Chinen, T. Kobayashi, T. Sato, A. Sakuraba, M. T. Kitazume, A. Sugita, K. Koganei, K. S. Akagawa, T. Hibi, Unique CD14 intestinal macrophages contribute to the pathogenesis of Crohn disease via IL-23/IFN-gamma axis. *J. Clin. Invest.* **118**, 2269–2280 (2008).
- Y. R. Na, M. Stakenborg, S. H. Seok, G. Matteoli, Macrophages in intestinal inflammation and resolution: A potential therapeutic target in IBD. *Nat. Rev. Gastroenterol. Hepatol.* **16**, 531–543 (2019).
- S. M. Bal, K. Golebski, H. Spits, Plasticity of innate lymphoid cell subsets. *Nat. Rev. Immunol.* 10.1038/s41577-020-0282-9, (2020).
- A. I. Lim, S. Menegatti, J. Bustamante, L. Le Bourhis, M. Allez, L. Rogge, J.-L. Casanova, H. Yssel, J. P. Di Santo, IL-12 drives functional plasticity of human group 2 innate lymphoid cells. *J. Exp. Med.* **213**, 569–583 (2016).
- L. Zhou, C. Chu, F. Teng, N. J. Bessman, J. Goc, E. K. Santosa, G. G. Putzel, H. Kabata, J. R. Kelsen, R. N. Baldassano, M. A. Shah, R. E. Sockolow, E. Vivier, G. Eberl, K. A. Smith, G. F. Sonnenberg, Innate lymphoid cells support regulatory T cells in the intestine through interleukin-2. *Nature* **568**, 405–409 (2019).
- J. Maul, C. Loddenkemper, P. Mundt, E. Berg, T. Giese, A. Stallmach, M. Zeitz, R. Duchmann, Peripheral and intestinal regulatory CD4+CD25^{high} T cells in inflammatory bowel disease. *Gastroenterology* **128**, 1868–1878 (2005).
- V. Mitsialis, S. Wall, P. Liu, J. Ordovas-Montanes, T. Parmet, M. Vukovic, D. Spencer, M. Field, C. McCourt, J. Toothaker, A. Bousvaros; Boston Children's Hospital Inflammatory Bowel Disease Center; Brigham and Women's Hospital Crohn's and Colitis Center, A. K. Shalek, L. Kean, B. Horwitz, J. Goldsmith, G. Tseng, S. B. Snapper, L. Konnikova, Single-cell analyses of colon and blood reveal distinct immune cell signatures of ulcerative colitis and Crohn's disease. *Gastroenterology* S0016-5085(20)30658-2, (2020).
- T. Ogino, J. Nishimura, S. Barman, H. Kayama, S. Uematsu, D. Okuzaki, H. Osawa, N. Haraguchi, M. Uemura, T. Hata, I. Takemasa, T. Mizushima, H. Yamamoto, K. Takeda, Y. Doki, M. Mori, Increased Th17-inducing activity of CD14⁺ CD163^{low} myeloid cells in intestinal lamina propria of patients with Crohn's disease. *Gastroenterology* **145**, 1380–1391.e1 (2013).
- J. Arsenio, B. Kakaradov, P. J. Metz, S. H. Kim, G. W. Yeo, J. T. Chang, Early specification of CD8⁺ T lymphocyte fates during adaptive immunity revealed by single-cell gene-expression analyses. *Nat. Immunol.* **15**, 365–372 (2014).
- B. Kakaradov, J. Arsenio, C. E. Widjaja, Z. He, S. Aigner, P. J. Metz, B. Yu, E. J. Wehrens, J. Lopez, S. H. Kim, E. I. Zuniga, A. W. Goldrath, J. T. Chang, G. W. Yeo, Early transcriptional and epigenetic regulation of CD8⁺ T cell differentiation revealed by single-cell RNA sequencing. *Nat. Immunol.* **18**, 422–432 (2017).
- K. Bahar Halpern, R. ShenHAV, O. Matcovitch-Natan, B. Tóth, D. Lemze, M. Golan, E. E. Massasa, S. Baydatch, S. Landen, A. E. Moor, A. Brandis, A. Giladi, A. Stokar-Avihail, E. David, I. Amit, S. Itzkovitz, Single-cell spatial reconstruction reveals global division of labour in the mammalian liver. *Nature* **542**, 352–356 (2017).
- B. Treutlein, D. G. Brownfield, A. R. Wu, N. F. Neff, G. L. Mantalas, F. H. Espinoza, T. J. Desai, M. A. Krasnow, S. R. Quake, Reconstructing lineage hierarchies of the distal lung epithelium using single-cell RNA-seq. *Nature* **509**, 371–375 (2014).

15. B. Treutlein, Q. Y. Lee, J. G. Camp, M. Mall, W. Koh, S. A. M. Shariati, S. Sim, N. F. Neff, J. M. Skotheim, M. Wernig, S. R. Quake, Dissecting direct reprogramming from fibroblast to neuron using single-cell RNA-seq. *Nature* **534**, 391–395 (2016).
16. A. Wagner, A. Regev, Revealing the vectors of cellular identity with single-cell genomics. *Nat. Biotechnol.* **34**, 1145–1160 (2016).
17. J. Kinchen, H. H. Chen, K. Parikh, A. Antanaviciute, M. Jagielowicz, D. Fawkner-Corbett, N. Ashley, L. Cubitt, E. Mellado-Gomez, M. Attar, E. Sharma, Q. Wills, R. Bowden, F. C. Richter, D. Ahern, K. D. Puri, J. Henault, F. Gervais, H. Koohy, A. Simmons, Structural remodeling of the human colonic mesenchyme in inflammatory bowel disease. *Cell* **175**, 372–386.e17 (2018).
18. J. C. Martin, C. Chang, G. Boschetti, R. Ungaro, M. Giri, J. A. Grout, K. Gettler, L.-s. Chuang, S. Nayar, A. J. Greenstein, M. Dubinsky, L. Walker, A. Leader, J. S. Fine, C. E. Whitehurst, M. L. Mbow, S. Kugathasan, L. A. Denson, J. S. Hyams, J. R. Friedman, P. T. Desai, H. M. Ko, I. Laface, G. Akturk, E. E. Schadt, H. Salmon, S. Gnajtic, A. H. Rahman, M. Merad, J. H. Cho, E. Kenigsberg, Single-cell analysis of Crohn's disease lesions identifies a pathogenic cellular module associated with resistance to anti-TNF therapy. *Cell* **178**, 1493–1508.e20 (2019).
19. C. S. Smillie, M. Biton, J. Ordovas-Montanes, K. M. Sullivan, G. Burgin, D. B. Graham, R. H. Herbst, N. Rogel, M. Slyper, J. Waldman, M. Sud, E. Andrews, G. Velonias, A. L. Haber, K. Jagadeesh, S. Vickovic, J. Yao, C. Stevens, D. Dionne, L. T. Nguyen, A.-C. Villani, M. Hofree, E. A. Creasey, H. Huang, O. Rozenblatt-Rosen, J. J. Garber, H. Khalili, A. N. Desch, M. J. Daly, A. N. Ananthakrishnan, A. K. Shalek, R. J. Xavier, A. Regev, Intra- and inter-cellular rewiring of the human colon during ulcerative colitis. *Cell* **178**, 714–730.e22 (2019).
20. K. Parikh, A. Antanaviciute, D. Fawkner-Corbett, M. Jagielowicz, A. Aulicino, C. Lagerholm, S. Davis, J. Kinchen, H. H. Chen, N. K. Alham, N. Ashley, E. Johnson, P. Hublitz, L. Bao, J. Lukomska, R. S. Andev, E. Björklund, B. M. Kessler, R. Fischer, R. Goldin, H. Koohy, A. Simmons, Colonic epithelial cell diversity in health and inflammatory bowel disease. *Nature* **567**, 49–55 (2019).
21. L. Zhang, X. Yu, L. Zheng, Y. Zhang, Y. Li, Q. Fang, R. Gao, B. Kang, Q. Zhang, J. Y. Huang, H. Konno, X. Guo, Y. Ye, S. Gao, S. Wang, X. Hu, X. Ren, Z. Shen, W. Ouyang, Z. Zhang, Lineage tracking reveals dynamic relationships of T cells in colorectal cancer. *Nature* **564**, 268–272 (2018).
22. L. D. Goldstein, Y.-J. J. Chen, J. Wu, S. Chaudhuri, Y.-C. Hsiao, K. Schneider, K. H. Hoi, Z. Lin, S. Guerrero, B. S. Jaiswal, J. Stinson, A. Antony, K. B. Pahuja, D. Seshasayee, Z. Modrusan, I. Hötzeli, S. Seshagiri, Massively parallel single-cell B-cell receptor sequencing enables rapid discovery of diverse antigen-reactive antibodies. *Commun. Biol.* **2**, 304 (2019).
23. L. K. Mackay, A. Kallies, Transcriptional regulation of tissue-resident lymphocytes. *Trends Immunol.* **38**, 94–103 (2017).
24. A. N. Hegazy, N. R. West, M. J. T. Stubbington, E. Wendt, K. I. M. Suijker, A. Datsi, S. This, C. Danne, S. Campion, S. H. Duncan, B. M. J. Owens, H. H. Uhlig, A. McMichael; Oxford IBD Cohort Investigators, A. Bergthaler, S. A. Teichmann, S. Keshav, F. Powrie, Circulating and tissue-resident CD4⁺ T cells with reactivity to intestinal microbiota are abundant in healthy individuals and function is altered during inflammation. *Gastroenterology* **153**, 1320–1337.e16 (2017).
25. S. Zundler, E. Becker, M. Spocinska, M. Slawik, L. Parga-Vidal, R. Stark, M. Wiendl, R. Atreya, T. Rath, M. Leppkes, K. Hildner, R. López-Posadas, S. Lukassen, A. B. Ekici, C. Neufert, I. Atreya, K. P. J. M. van Gisbergen, M. F. Neurath, Hobit- and Blimp1-driven CD4⁺ tissue-resident memory T cells control chronic intestinal inflammation. *Nat. Immunol.* **20**, 288–300 (2019).
26. S. Z. Josefowicz, L.-F. Lu, A. Y. Rudensky, Regulatory T cells: Mechanisms of differentiation and function. *Annu. Rev. Immunol.* **30**, 531–564 (2012).
27. S. Crotty, T follicular helper cell biology: A decade of discovery and diseases. *Immunity* **50**, 1132–1148 (2019).
28. A. N. Keller, A. J. Corbett, J. M. Wubben, J. McCluskey, J. Rossjohn, MAIT cells and MR1-antigen recognition. *Curr. Opin. Immunol.* **46**, 66–74 (2017).
29. M. Beyer, Y. Thabet, R.-U. Müller, T. Sadlon, S. Classen, K. Lahli, S. Basu, X. Zhou, S. L. Bailey-Bucktrout, W. Krebs, E. A. Schönfeld, J. Böttcher, T. Golovina, C. T. Mayer, A. Hofmann, D. Sommer, S. Debey-Pascher, E. Endl, A. Limmer, K. L. Hippchen, B. R. Blazquez, R. Balderas, T. Quast, A. Waha, G. Mayer, M. Famulok, P. A. Knolle, C. Wickenhauser, W. Kolanus, B. Schermer, J. A. Bluestone, S. C. Barry, T. Sparwasser, J. L. Riley, J. L. Schultze, Repression of the genome organizer SATB1 in regulatory T cells is required for suppressive function and inhibition of effector differentiation. *Nat. Immunol.* **12**, 898–907 (2011).
30. Y. Kitagawa, N. Ohkura, Y. Kidani, A. Vandenberg, K. Hirota, R. Kawakami, K. Yasuda, D. Motooka, S. Nakamura, M. Kondo, I. Taniuchi, T. Kohwi-Shigematsu, S. Sakaguchi, Guidance of regulatory T cell development by Satb1-dependent super-enhancer establishment. *Nat. Immunol.* **18**, 173–183 (2017).
31. J. E. Klann, S. H. Kim, K. A. Remedios, Z. He, P. J. Metz, J. Lopez, T. Tysl, J. G. Olvera, J. N. Ablack, J. M. Cantor, B. S. Boland, G. Yeo, Y. Zheng, L.-F. Lu, J. D. Bui, M. H. Ginsberg, B. G. Petrich, J. T. Chang, Integrin activation controls regulatory T cell-mediated peripheral tolerance. *J. Immunol.* **200**, 4012–4023 (2018).
32. S. K. Pabbiisetty, W. Rabacal, D. Maseda, D. Cendron, P. L. Collins, K. L. Hoek, V. V. Parekh, T. M. Aune, E. Sebzda, KLF2 is a rate-limiting transcription factor that can be targeted to enhance regulatory T-cell production. *Proc. Natl. Acad. Sci. U.S.A.* **111**, 9579–9584 (2014).
33. J. Saravia, H. Zeng, Y. Dhungana, D. Bastardo Blanco, T.-L. M. Nguyen, N. M. Chapman, Y. Wang, A. Kanneganti, S. Liu, J. L. Raynor, P. Vogel, G. Neale, P. Carmeliet, H. Chi, Homeostasis and transitional activation of regulatory T cells require c-Myc. *Sci. Adv.* **6**, eaaw6443 (2020).
34. C. X. Dominguez, R. A. Amezquita, T. Guan, H. D. Marshall, N. S. Joshi, S. H. Kleinstein, S. M. Kaech, The transcription factors ZEB2 and T-bet cooperate to program cytotoxic T cell terminal differentiation in response to LCMV viral infection. *J. Exp. Med.* **212**, 2041–2056 (2015).
35. K. D. Omilusik, J. A. Best, B. Yu, S. Goossens, A. Weidemann, J. V. Nguyen, E. Seuntjens, A. Stryjewska, C. Zweier, R. Roychoudhuri, L. Gattinoni, L. M. Bird, Y. Higashi, H. Kondoh, D. Huylebroeck, J. Haigh, A. W. Goldrath, Transcriptional repressor ZEB2 promotes terminal differentiation of CD8⁺ effector and memory T cell populations during infection. *J. Exp. Med.* **212**, 2027–2039 (2015).
36. Y. Pan, T. Tian, C. O. Park, S. Y. Loftus, S. Mei, X. Liu, C. Luo, J. T. O'Malley, A. Gehad, J. E. Teague, S. J. Divito, R. Fuhlbrigge, P. Puigserver, J. G. Krueger, G. S. Hotamisligil, R. A. Clark, T. S. Kupper, Survival of tissue-resident memory T cells requires exogenous lipid uptake and metabolism. *Nature* **543**, 252–256 (2017).
37. E. L. Pearce, A. C. Mullen, G. A. Martins, C. M. Krawczyk, A. S. Hutchins, V. P. Zediak, M. Banica, C. B. DiCioccio, D. A. Gross, C.-a. Mao, H. Shen, N. Cereb, S. Y. Yang, T. Lindsten, J. Rossant, C. A. Hunter, S. L. Reiner, Control of effector CD8⁺ T cell function by the transcription factor Eomesodermin. *Science* **302**, 1041–1043 (2003).
38. J. T. Chang, E. J. Wherry, A. W. Goldrath, Molecular regulation of effector and memory T cell differentiation. *Nat. Immunol.* **15**, 1104–1115 (2014).
39. J. Li, Y. He, J. Hao, L. Ni, C. Dong, High levels of eomes promote exhaustion of anti-tumor CD8⁺ T cells. *Front. Immunol.* **9**, 2981 (2018).
40. K. Holgersen, P. H. Kvist, H. Markholst, A. K. Hansen, T. L. Holm, Characterisation of enterocolitis in the piroxicam-accelerated interleukin-10 knock out mouse—A model mimicking inflammatory bowel disease. *J. Crohns Colitis* **8**, 147–160 (2014).
41. S. Punit, P. E. Dube, C. Y. Liu, N. Girish, M. K. Washington, D. B. Polk, Tumor necrosis factor receptor 2 restricts the pathogenicity of CD8⁺ T cells in mice with colitis. *Gastroenterology* **149**, 993–1005.e2 (2015).
42. N. Istance, M. Splittergerber, V. Lima Silva, M. Nguyen, S. Thomas, A. Le, Y. Achouri, E. Calonne, M. Defrance, F. Fuks, S. Goriely, A. Azouz, EOMES interacts with RUNX3 and BRG1 to promote innate memory cell formation through epigenetic reprogramming. *Nat. Commun.* **10**, 3306 (2019).
43. J. J. Milner, C. Toma, B. Yu, K. Zhang, K. Omilusik, A. T. Phan, D. Wang, A. J. Getzler, T. Nguyen, S. Crotty, W. Wang, M. E. Pipkin, A. W. Goldrath, Runx3 programs CD8⁺ T cell residency in non-lymphoid tissues and tumours. *Nature* **552**, 253–257 (2017).
44. P. Brandtzaeg, K. Baklien, O. Fausa, P. S. Hoel, Immunohistochemical characterization of local immunoglobulin formation in ulcerative colitis. *Gastroenterology* **66**, 1123–1136 (1974).
45. T. Castro-Dopico, T. W. Dennison, J. R. Ferdinand, R. J. Mathews, A. Fleming, D. Clift, B. J. Stewart, C. Jing, K. Strongili, L. I. Labzin, E. J. M. Monk, K. Saeb-Parsy, C. E. Bryant, S. Clare, M. Parkes, M. R. Clatworthy, Anti-commensal IgG drives intestinal inflammation and Type 17 immunity in ulcerative colitis. *Immunity* **50**, 1099–1114.e10 (2019).
46. A. Macpherson, U. Y. Khoo, I. Forgacs, J. Philpott-Howard, I. Bjarnason, Mucosal antibodies in inflammatory bowel disease are directed against intestinal bacteria. *Gut* **38**, 365–375 (1996).
47. M. Uo, T. Hisamatsu, J. Miyoshi, D. Kaito, K. Yoneno, M. T. Kitazume, M. Mori, A. Sugita, K. Koganei, K. Matsuoka, T. Kanai, T. Hibi, Mucosal CXCR4⁺ IgG plasma cells contribute to the pathogenesis of human ulcerative colitis through FcγR-mediated CD14 macrophage activation. *Gut* **62**, 1734–1744 (2013).
48. N. W. Palm, M. R. de Zoete, T. W. Cullen, N. A. Barry, J. Stefanowski, L. Hao, P. H. Degnan, J. Hu, I. Peter, W. Zhang, E. Ruggiero, J. H. Cho, A. L. Goodman, R. A. Flavell, Immunoglobulin A coating identifies colitogenic bacteria in inflammatory bowel disease. *Cell* **158**, 1000–1010 (2014).
49. N. S. Kurd, Z. He, T. L. Louis, J. J. Milner, K. D. Omilusik, W. Jin, M. S. Tsai, C. E. Widjaja, J. N. Kanbar, J. G. Olvera, T. Tysl, L. K. Quezada, B. S. Boland, W. J. Huang, C. Murre, A. W. Goldrath, G. W. Yeo, J. T. Chang, Early precursors and molecular determinants of tissue-resident memory CD8⁺ T lymphocytes revealed by single-cell RNA sequencing. *Sci. Immunol.* **5**, eaaz6894 (2020).
50. J. J. Milner, C. Toma, Z. He, N. S. Kurd, Q. P. Nguyen, B. McDonald, L. Quezada, C. E. Widjaja, D. A. Witherden, J. T. Crowl, L. A. Shaw, G. W. Yeo, J. T. Chang, K. D. Omilusik, A. W. Goldrath, Heterogenous populations of tissue-resident CD8⁺ T cells are generated in response to infection and malignancy. *Immunity* **52**, 808–824.e7 (2020).
51. B. V. Kumar, R. Kratchmarov, M. Miron, D. J. Carpenter, T. Senda, H. Lerner, A. Friedman, S. L. Reiner, D. L. Farber, Functional heterogeneity of human tissue-resident memory T cells based on dye efflux capacities. *JCI Insight* **3**, e123568 (2018).

52. S. Cheuk, H. Schlums, I. Gallais Séréal, E. Martini, S. C. Chiang, N. Marquardt, A. Gibbs, E. Detlöfsson, A. Introini, M. Forkel, C. Höög, A. Tjernlund, J. Michaëlsson, L. Folkersen, J. Mjösberg, L. Blomqvist, M. Ehrström, M. Stähle, Y. T. Bryceon, L. Eidsmo, CD49a expression defines tissue-resident CD8⁺ T cells poised for cytotoxic function in human skin. *Immunity* **46**, 287–300 (2017).
53. R. A. Clark, Resident memory T cells in human health and disease. *Sci. Transl. Med.* **7**, 269rv1 (2015).
54. R. Fonseca, L. K. Beura, C. F. Quarnstrom, H. E. Ghoneim, Y. Fan, C. C. Zebley, M. C. Scott, N. J. Fares-Frederickson, S. Wijeyesinghe, E. A. Thompson, H. Borges da Silva, V. Vezys, B. Youngblood, D. Masopust, Developmental plasticity allows outside-in immune responses by resident memory T cells. *Nat. Immunol.* **21**, 412–421 (2020).
55. M. M. Klicznik, P. A. Morawski, B. Höllbacher, S. R. Varkhande, S. J. Motley, L. Kuri-Cervantes, E. Goodwin, M. D. Rosenblum, S. A. Long, G. Bracht, T. Duhen, M. R. Betts, D. J. Campbell, I. K. Gratz, Human CD4⁺CD103⁺ cutaneous resident memory T cells are found in the circulation of healthy individuals. *Sci. Immunol.* **4**, eaav8995 (2019).
56. A. M. Intlekofer, N. Takemoto, E. J. Wherry, S. A. Longworth, J. T. Northrup, V. R. Palanivel, A. C. Mullen, C. R. Gasink, S. M. Kaech, J. D. Miller, L. Gapin, K. Ryan, A. P. Russ, T. Lindsten, J. S. Orange, A. W. Goldrath, R. Ahmed, S. L. Reiner, Effector and memory CD8⁺ T cell fate coupled by T-bet and eomesodermin. *Nat. Immunol.* **6**, 1236–1244 (2005).
57. T. C. Becker, E. J. Wherry, D. Boone, K. Murali-Krishna, R. Antia, A. Ma, R. Ahmed, Interleukin 15 is required for proliferative renewal of virus-specific memory CD8 T cells. *J. Exp. Med.* **195**, 1541–1548 (2002).
58. A. W. Goldrath, P. V. Sivakumar, M. Glaccum, M. K. Kennedy, M. J. Bevan, C. Benoist, D. Mathis, E. A. Butz, Cytokine requirements for acute and basal homeostatic proliferation of naive and memory CD8⁺ T cells. *J. Exp. Med.* **195**, 1515–1522 (2002).
59. A. Banerjee, S. M. Gordon, A. M. Intlekofer, M. A. Paley, E. C. Mooney, T. Lindsten, E. J. Wherry, S. L. Reiner, Cutting edge: The transcription factor eomesodermin enables CD8⁺ T cells to compete for the memory cell niche. *J. Immunol.* **185**, 4988–4992 (2010).
60. M. A. Paley, D. C. Kroy, P. M. Odorizzi, J. B. Johnnidis, D. V. Dolfi, B. E. Barnett, E. K. Bikoff, E. J. Robertson, G. M. Lauer, S. L. Reiner, E. J. Wherry, Progenitor and terminal subsets of CD8⁺ T cells cooperate to contain chronic viral infection. *Science* **338**, 1220–1225 (2012).
61. L. K. Mackay, A. Rahimpour, J. Z. Ma, N. Collins, A. T. Stock, M.-L. Hafon, J. Vega-Ramos, P. Lauzurica, S. N. Mueller, T. Stefanovic, D. C. Tscharke, W. R. Heath, M. Inouye, F. R. Carbone, T. Gebhardt, The developmental pathway for CD103⁺CD8⁺ tissue-resident memory T cells of skin. *Nat. Immunol.* **14**, 1294–1301 (2013).
62. B. J. Laidlaw, N. Zhang, H. D. Marshall, M. M. Staron, T. Guan, Y. Hu, L. S. Cauley, J. Craft, S. M. Kaech, CD4⁺ T cell help guides formation of CD103⁺ lung-resident memory CD8⁺ T cells during influenza viral infection. *Immunity* **41**, 633–645 (2014).
63. L. M. Wakim, A. Woodward-Davis, R. Liu, Y. Hu, J. Villadangos, G. Smyth, M. J. Bevan, The molecular signature of tissue resident memory CD8 T cells isolated from the brain. *J. Immunol.* **189**, 3462–3471 (2012).
64. K. S. Boles, W. Barchet, T. Diacovo, M. Cella, M. Colonna, The tumor suppressor TSLC1/NECL-2 triggers NK-cell and CD8⁺ T-cell responses through the cell-surface receptor CRTAM. *Blood* **106**, 779–786 (2005).
65. Y. Higashi, M. Maruhashi, L. Nelles, T. Van de Putte, K. Verschueren, T. Miyoshi, A. Yoshimoto, H. Kondoh, D. Huylebroeck, Generation of the floxed allele of the SIP1 (Smad-interacting protein 1) gene for Cre-mediated conditional knockout in the mouse. *Genesis* **32**, 82–84 (2002).
66. R. Hess Michelini, A. L. Doedens, A. W. Goldrath, S. M. Hedrick, Differentiation of CD8 memory T cells depends on Foxo1. *J. Exp. Med.* **210**, 1189–1200 (2013).
67. T. D. Wu, S. Madireddi, P. E. de Almeida, R. Banchereau, Y.-J. Chen, A. S. Chitre, E. Y. Chiang, H. Iftikhar, W. E. O'Gorman, A. Au-Yeung, C. Takahashi, L. D. Goldstein, C. Poon, S. Keerthivasan, D. E. de Almeida Nagata, X. Du, H.-M. Lee, K. L. Banta, S. Mariathasan, M. Das Thakur, M. A. Huseni, M. Ballinger, I. Estay, P. Caplazi, Z. Modrusan, L. Delamarre, I. Mellman, R. Bourgon, J. L. Grogan, Peripheral T cell expansion predicts tumour infiltration and clinical response. *Nature* **579**, 274–278 (2020).
68. D. Troutaud, M. Drouet, C. Decourt, C. Le Morvan, M. Cogné, Age-related alterations of somatic hypermutation and CDR3 lengths in human Vκ4-expressing B lymphocytes. *Immunology* **97**, 197–203 (1999).
69. D. Koning, A. I. Costa, I. Hoof, J. J. Miles, N. M. Nanlohy, K. Ladell, K. K. Matthews, V. Venturi, I. M. M. Schellens, J. A. M. Borghans, C. Keşmir, D. A. Price, D. van Baarle, CD8⁺ TCR repertoire formation is guided primarily by the peptide component of the antigenic complex. *J. Immunol.* **190**, 931–939 (2013).
70. D. Rissó, J. Ngai, T. P. Speed, S. Dudoit, Normalization of RNA-seq data using factor analysis of control genes or samples. *Nat. Biotechnol.* **32**, 896–902 (2014).
71. E. Eisenberg, E. Y. Levanon, Human housekeeping genes, revisited. *Trends Genet.* **29**, 569–574 (2013).
72. A. Butler, P. Hoffman, P. Smibert, E. Papalexi, R. Satija, Integrating single-cell transcriptomic data across different conditions, technologies, and species. *Nat. Biotechnol.* **36**, 411–420 (2018).
73. M. D. Luecken, F. J. Theis, Current best practices in single-cell RNA-seq analysis: A tutorial. *Mol. Syst. Biol.* **15**, e8746 (2019).
74. M. I. Love, W. Huber, S. Anders, Moderated estimation of fold change and dispersion for RNA-seq data with DESeq2. *Genome Biol.* **15**, 550 (2014).
75. D. Rissó, F. Perraudau, S. Gribkova, S. Dudoit, J.-P. Vert, A general and flexible method for signal extraction from single-cell RNA-seq data. *Nat. Commun.* **9**, 284 (2018).

Acknowledgments: We thank L. Arambula Tsai for assistance with figures. We thank members of the Chang, Goldrath, and Yeo laboratories for technical advice, helpful discussion, and critical reading of the manuscript. scRNA-seq, TCR-seq, and BCR-seq using the 10x Genomics platform were performed at the UCSD IGM Genomics Center and supported by NIH grants P30KC063491, P30CA023100, and S10OD026929. Microscopy was performed at the UCSD Microscopy Core and supported by NIH grant NS047101. Mass cytometry was performed at the La Jolla Institute for Immunology Flow Cytometry Core and supported by NIH grant S10OD018499. **Funding:** This work was supported by the NIDDK-funded San Diego Digestive Diseases Research Center (P30DK120515) and the CCSG grant (P30CA23100) and funded by grants from the Kenneth Rainin Foundation (W.J.S., G.W.Y., and J.T.C.) and the NIH: TR001444 and DK123406 (B.S.B.); DK007202 (M.S.T.); AI08280 and AI00880; AI123202, AI129973, and BX003424 (J.T.C.); AI132122 (A.W.G., G.W.Y., and J.T.C.); and MH107367 (G.W.Y.).

Author contributions: G.W.Y. and J.T.C. conceived the study. B.S.B., Z.H., M.S.T., J.G.O., K.D.O., W.J., H.G.D., E.S.K., A.E.L., T.T., J.J.M., B.Y., S.A.P., T.L.L., N.S.K., A.B., L.K.Q., J.N.K., A.M., P.S.D., and S.S. performed data acquisition, analysis, or interpretation. D.H., M.A.V., C.M., L.-F.L., J.D.B., W.J.S., A.W.G., G.W.Y., and J.T.C. supervised the study. B.S.B., Z.H., M.S.T., G.W.Y., and J.T.C. wrote and edited the manuscript. **Competing interests:** B.S.B. was a consultant for AbbVie, Prometheus Laboratories, and Pfizer in the past 3 years. P.S.D. is on the steering committee for Takeda, is a consultant for Takeda and Janssen, and has received honoraria for speaker events from Takeda, travel support from Takeda and Janssen, and grant support from Takeda and Pfizer. G.W.Y. is cofounder, member of the Board of Directors, on the Science Advisory Boards (SAB), equity holder, and paid consultant for Locanabio and Eclipse BioInnovations. A.W.G. is on the SAB of Pandion Therapeutics and ArsenalBio. W.J.S. reports research grants from Atlantic Healthcare Limited, Amgen, Genentech, Gilead Sciences, AbbVie, Janssen, Takeda, Eli Lilly, Celgene/Receptos, Pfizer, and Prometheus Laboratories (now Prometheus Biosciences); consulting fees from AbbVie, Allergan, Amgen, Arena Pharmaceuticals, Avexegen Therapeutics, BeiGene, Boehringer Ingelheim, Celgene, Celltrion, Conatus, Cosmo, Escalier Biosciences, Ferring, Forbion, Genentech, Gilead Sciences, Gossamer Bio, Incyte, Janssen, Kyowa Kirin Pharmaceutical Research, Landos Biopharma, Eli Lilly, Oppilana Pharma, Otsuka, Pfizer, Progenity, Prometheus Biosciences (merger of Precision IBD and Prometheus Laboratories), Reistone, Ritter Pharmaceuticals, Robarts Clinical Trials [owned by Health Academic Research Trust (HART)], Series Therapeutics, Shire, Sienna Biopharmaceuticals, Sigmoid Biotechnologies, Stern Biologicals, Sublimity Therapeutics, Takeda, Theravance Biopharma, Tigenix, Tillotts Pharma, UCB Pharma, Ventyx Biosciences, Vimanan Biosciences, and Vivelix Pharmaceuticals; and stock or stock options from BeiGene, Escalier Biosciences, Gossamer Bio, Oppilana Pharma, Prometheus Biosciences (merger of Precision IBD and Prometheus Laboratories), Progenity, Ritter Pharmaceuticals, Shoreline Biosciences, Ventyx Biosciences, and Vimanan Biosciences. Spouse: Iveric Bio, consultant on stock options; Progenity, consultant on stock; Oppilana Pharma, consultant on stock options; Escalier Biosciences, prior employee (stock options); Prometheus Biosciences (merger of Precision IBD and Prometheus Laboratories), employee (stock options); Shoreline Biosciences, stock options; Ventyx Biosciences, stock options; and Vimanan Biosciences, stock options. J.T.C. reports research grant support from Takeda and Eli Lilly.

Data and materials availability: The data have been deposited in the Gene Expression Omnibus under accession number GSE125527. All other data needed to evaluate the conclusions in the paper are present in the paper or the Supplementary Materials.

Submitted 25 February 2020

Accepted 24 July 2020

Published 21 August 2020

10.1126/sciimmunol.abb4432

Citation: B. S. Boland, Z. He, M. S. Tsai, J. G. Olvera, K. D. Omilusik, H. G. Duong, E. S. Kim, A. E. Limary, W. Jin, J. J. Milner, B. Yu, S. A. Patel, T. L. Louis, T. Tysl, N. S. Kurd, A. Bortnick, L. K. Quezada, J. N. Kanbar, A. Miralles, D. Huylebroeck, M. A. Valasek, P. S. Dulai, S. Singh, L.-F. Lu, J. D. Bui, C. Murre, W. J. Sandborn, A. W. Goldrath, G. W. Yeo, J. T. Chang, Heterogeneity and clonal relationships of adaptive immune cells in ulcerative colitis revealed by single-cell analyses. *Sci. Immunol.* **5**, eabb4432 (2020).

Heterogeneity and clonal relationships of adaptive immune cells in ulcerative colitis revealed by single-cell analyses

Brigid S. Boland, Zhaoren He, Matthew S. Tsai, Jocelyn G. Olvera, Kyla D. Omilusik, Han G. Duong, Eleanor S. Kim, Abigail E. Limary, Wenhao Jin, J. Justin Milner, Bingfei Yu, Shefali A. Patel, Tiani L. Louis, Tiffani Tysl, Nadia S. Kurd, Alexandra Bortnick, Lauren K. Quezada, Jad N. Kanbar, Ara Miralles, Danny Huylebroeck, Mark A. Valasek, Parambir S. Dulai, Siddharth Singh, Li-Fan Lu, Jack D. Bui, Cornelis Murre, William J. Sandborn, Ananda W. Goldrath, Gene W. Yeo and John T. Chang

Sci. Immunol. **5**, eabb4432.
DOI: 10.1126/sciimmunol.abb4432

Profiles of rogue gut lymphocytes

Dysregulated human gut B and T lymphocytes contribute to the immunopathogenesis of ulcerative colitis (UC), a type of inflammatory bowel disease (IBD) characterized by mucosal damage in the colon. Boland *et al.* probed the immunologic perturbations associated with active UC by sequencing mRNA and clonal antigen receptors from individual CD45⁺ cells isolated from rectal biopsies or blood of patients and healthy controls. The resulting single-cell sequencing resource revealed heterogeneity among tissue-resident memory T cells (T_{RM}) in UC, including expansion of an inflammatory CD8⁺ T_{RM} subset expressing the Eomesodermin transcription factor. The identification of this T_{RM} population and other disease-associated T and B cell subsets provides a platform for future functional studies addressing how these subsets conspire to trigger chronic mucosal injury in UC.

ARTICLE TOOLS

<http://immunology.science.org/content/5/50/eabb4432>

SUPPLEMENTARY MATERIALS

<http://immunology.science.org/content/suppl/2020/08/17/5.50.eabb4432.DC1>

REFERENCES

This article cites 73 articles, 21 of which you can access for free
<http://immunology.science.org/content/5/50/eabb4432#BIBL>

Use of this article is subject to the [Terms of Service](#)

Science Immunology (ISSN 2470-9468) is published by the American Association for the Advancement of Science, 1200 New York Avenue NW, Washington, DC 20005. The title *Science Immunology* is a registered trademark of AAAS.

Copyright © 2020 The Authors, some rights reserved; exclusive licensee American Association for the Advancement of Science. No claim to original U.S. Government Works